ZCO 80: Zinc Effects on Mechanical Behaviour of AHSS Welds

October 19, 2017

Erica Wintjes, Hadi Razmpoosh, Andrew Macwan, Chris DiGiovanni, Xu Han, Norman Zhou

UNIVERSITY OF WATERLOO

Outline

- Project Objectives
- Resistance Spot Welding
  - Materials and Methods
  - Results and discussion
- Fiber Laser Welding
  - Material and Methods
  - Results and discussion
- Future Work

Project Objectives

- Develop understanding of the susceptibility of AHSS to LME through **thermomechanical testing of various zinc coating compositions**
- Evaluate the effect of various microstructural attributes such as **content of retained austenite, grain size, grain distribution, and alloying elements** on susceptibility to LME
- Investigate in detail the contribution thresholds of **different welding parameters and welding conditions**
- Experimentally quantify and validate **numerical models** of the stress fields present at the joint
- Correlate the mechanical properties to the onset of LME in AHSS welds with respect to **tensile and fatigue properties** at room temperature
- Develop guidelines for the **mitigation and remediation** of LME cracks in AHSS during RSW and laser welding

UNIVERSITY OF WATERLOO

Resistance spot welding

Materials

Material	Gauge (mm)	C	Mn	Mo	Si	P	Al	Cr	B
DP980-GI	1.20	0.15	1.5	-	0.3	-	0.05	-	-
DP980-GA	1.20	0.10	2.2	0.2	0.3	-	0.04	0.2	-
Med Mn-GI	1.45	0.15	10.4	-	0.17	-	1.49	-	-

Material	Coating Weight (g/m²)			Chemistry (wt%)		
	Top	Bottom	Total	Al	Fe	Zn
DP980-GI	60	55	115	-	0.03	Balance
DP980-GA	41	55	96	-	11	Balance
Med Mn-GI	50	50	100	~0.2	-	Balance

Welding Equipment and Parameters

- Max current: 60 kA
- Max force: 25 kN

- Welding Parameters for DP980 (AWS D8.9)
  - Force: 4 kN
  - Cooling: 4 L/min
  - Single Pulse (16 cy)
- Welding Parameters for MMn (AWS D8.9)
  - Force: 5 kN
  - Cooling: 6 L/min
  - Double Pulse (10-2-10 cy)

Sample Preparation

- For each condition, 3 samples were prepared for crack analysis and nugget diameter
- Procedure:

1. Examine samples for surface cracks and cross-section
2. Mount, grind, polish and etch samples
3. Measure cracks using optical microscopy
4. No. of cracks, total crack length, and Max. crack length

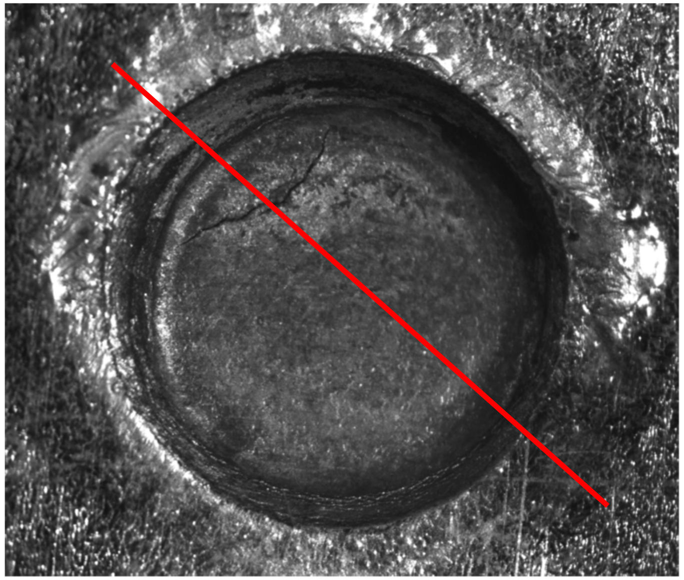

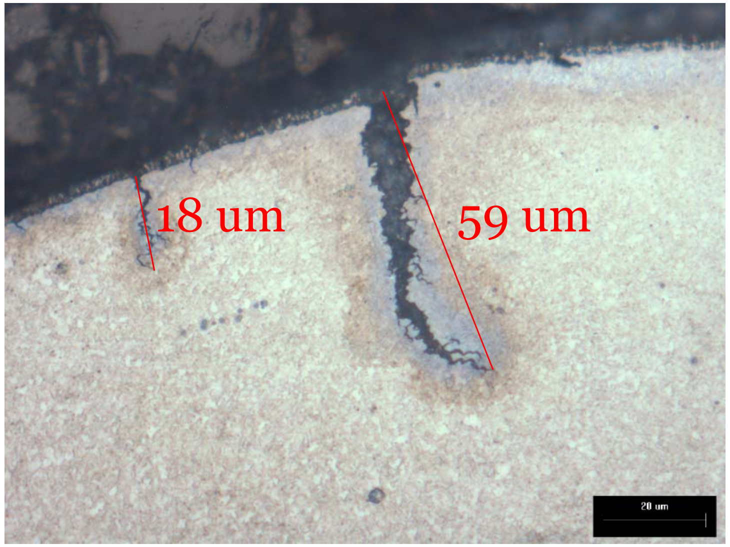

Welding Current and Time – DP980GI

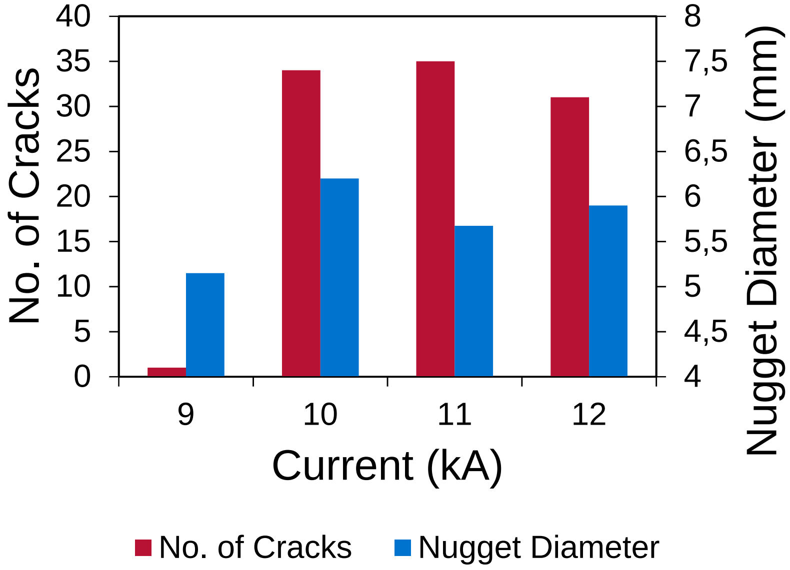

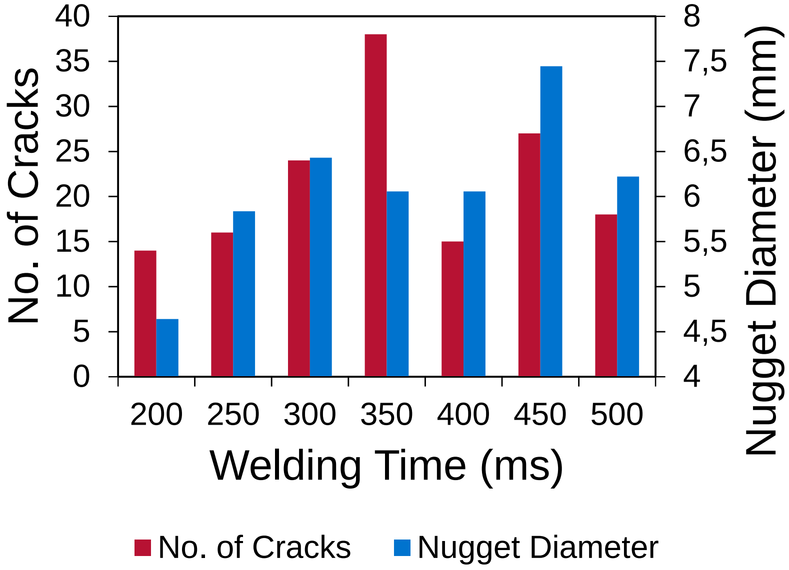

- Nugget diameter increases with increasing heat input (current and time)
- Number of cracks increases with increasing current
- Number of cracks increases with increasing weld time until 350 ms, where it decreases again

Welding Current and Time – DP980GI

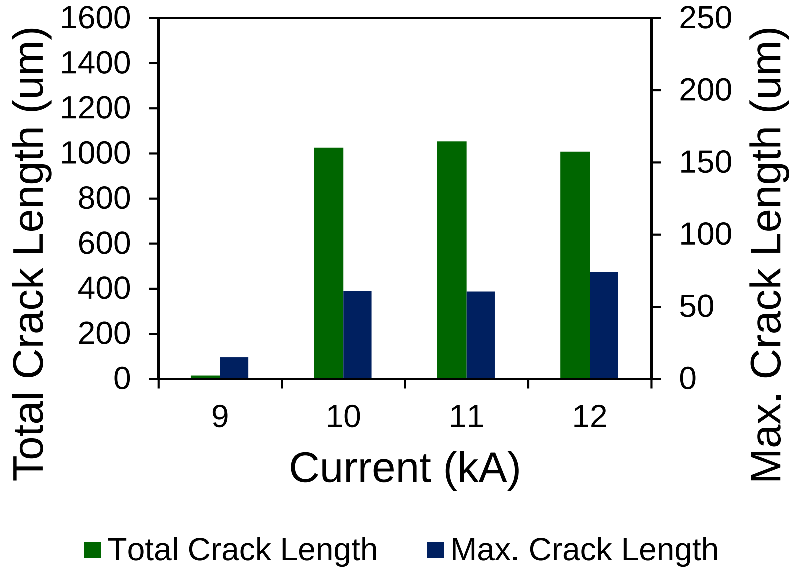

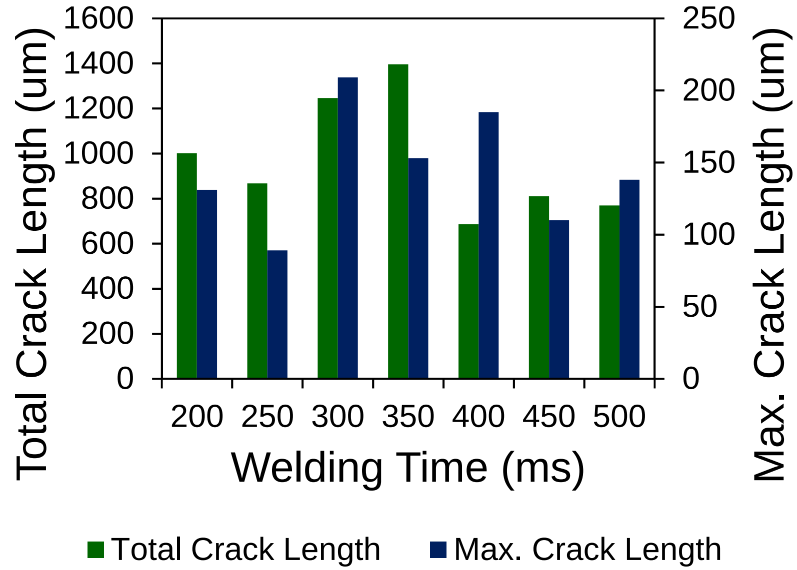

- Total and maximum crack lengths increase with increasing current
- Maximum crack length increases with increasing welding time until 300 ms, where it decreases again
  - Total crack length displays similar trend (peak located at 350 ms)

Process Maps – DP980GI

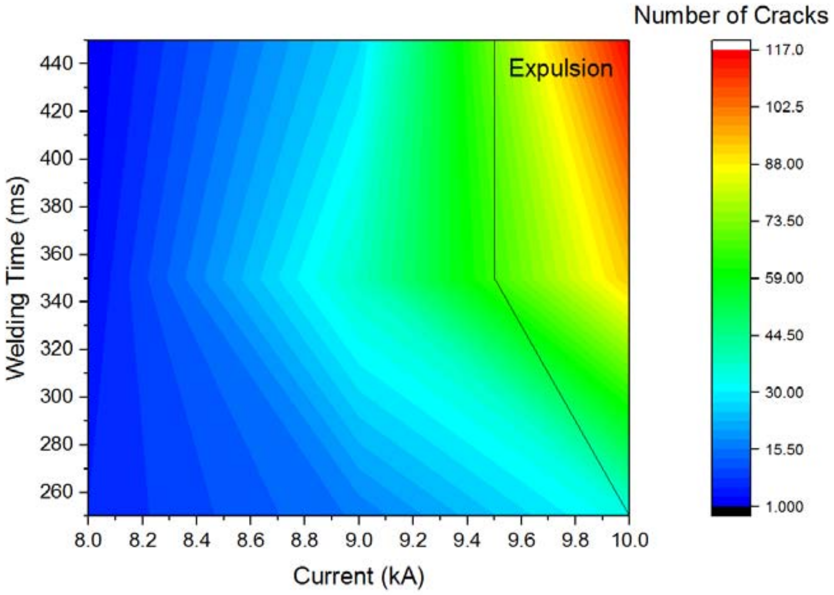

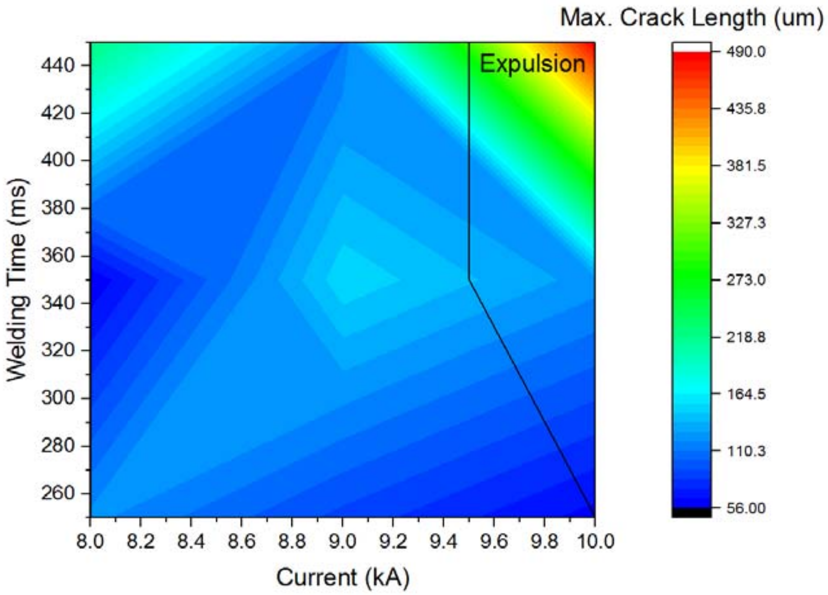

- Most cracking occurs at highest welding current and time
- Data for maximum crack length is somewhat scattered but still shows highest cracking at top right of map

UNIVERSITY OF WATERLOO

Welding Current and Time – DP980GA

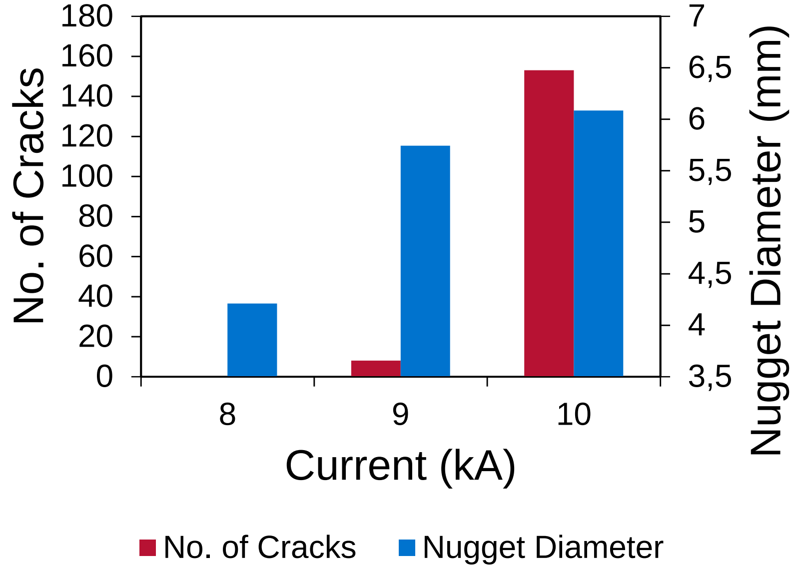

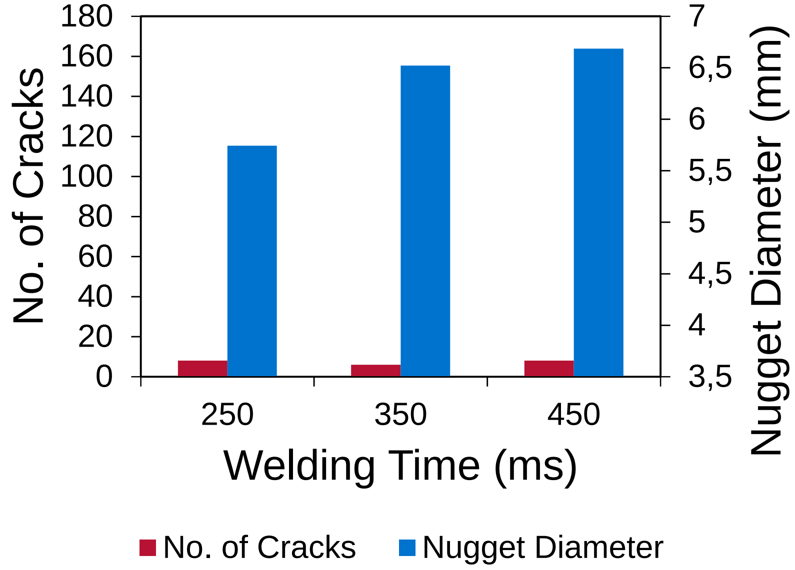

- Nugget diameter increases with increasing current and welding time
- Current has a larger effect on cracking than welding time
    - Significant cracking begins at 10 kA current

Welding Current and Time – DP980GA

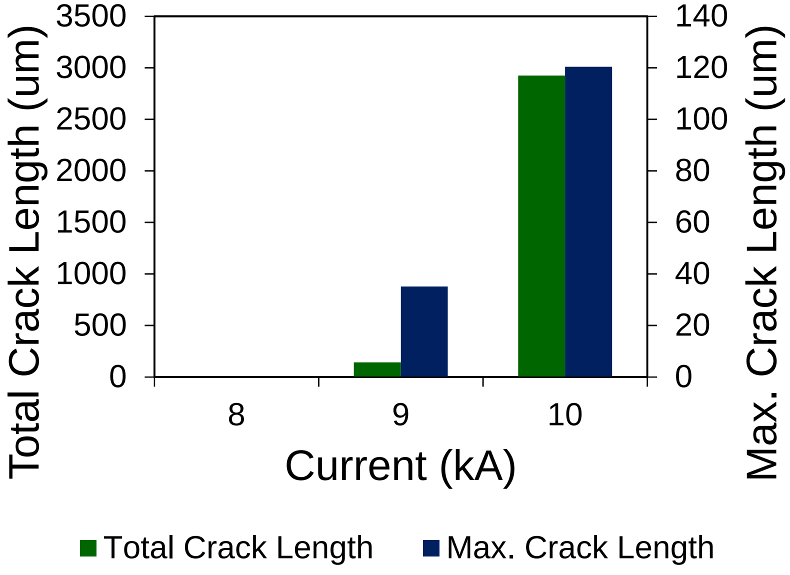

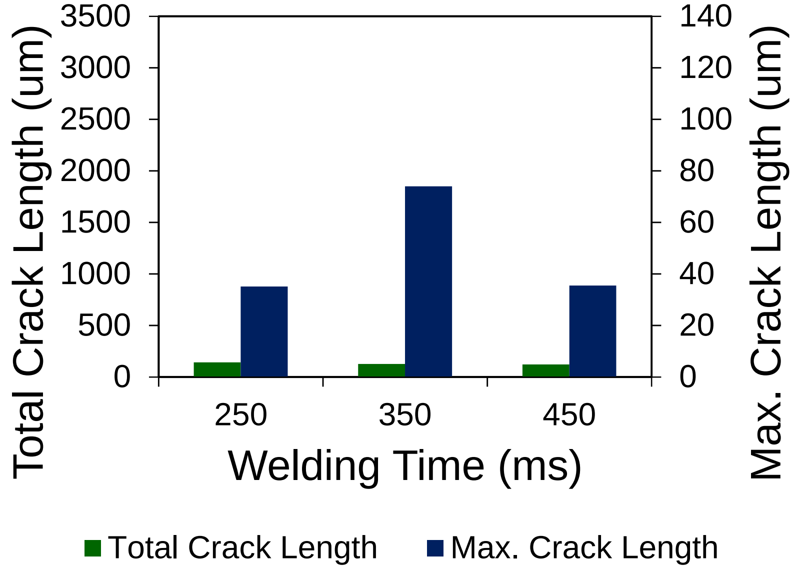

- Total and maximum crack lengths increase with increasing current
- No significant increasing trend in cracking with welding time

Process Maps – DP980GA

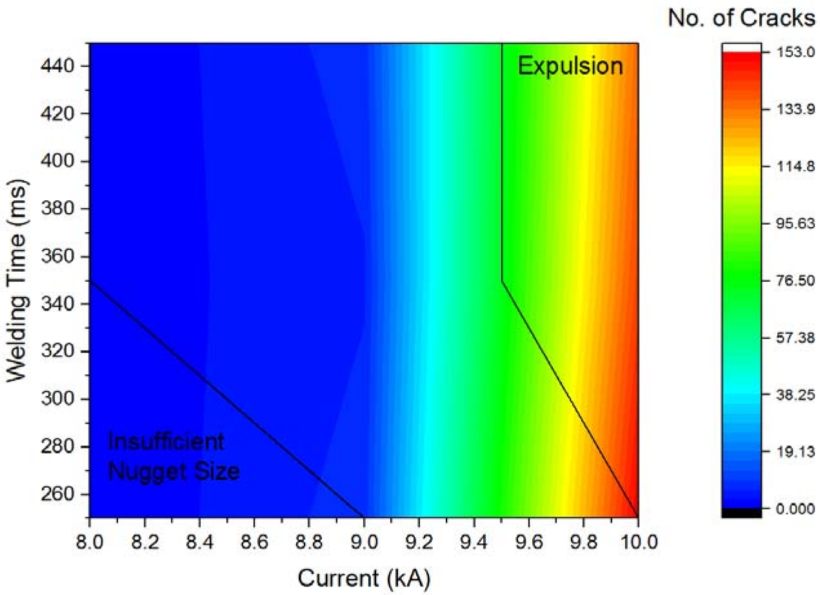

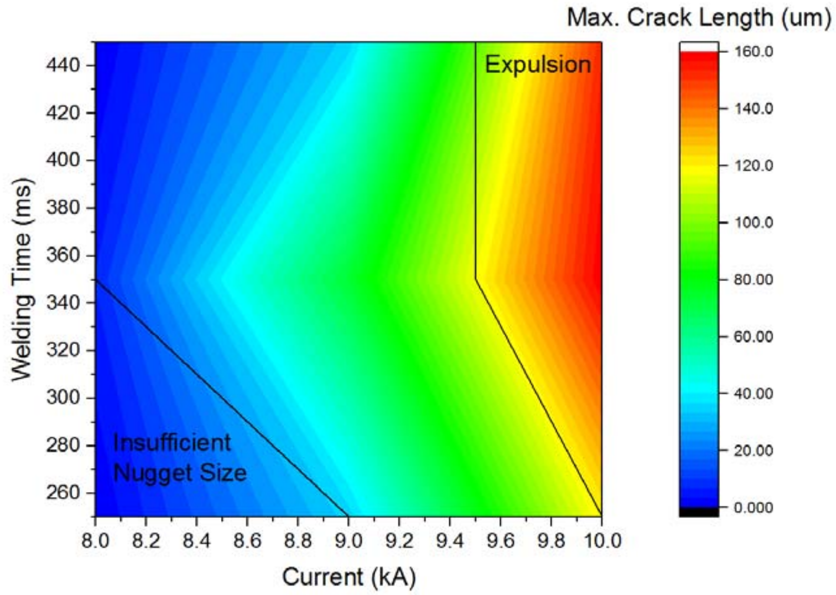

- Again, greatest cracking occurs at highest currents and times
- Current appears to have a greater effect on cracking than welding time

DP980 – GA vs GI coating

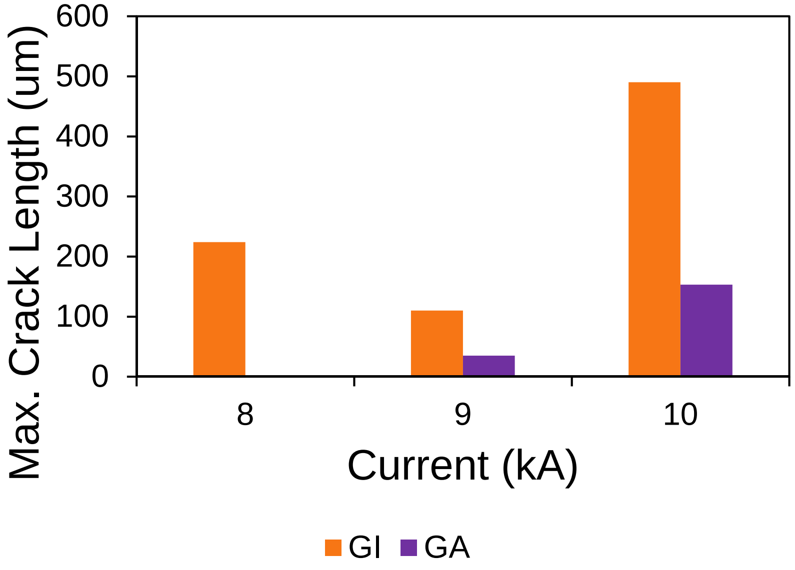

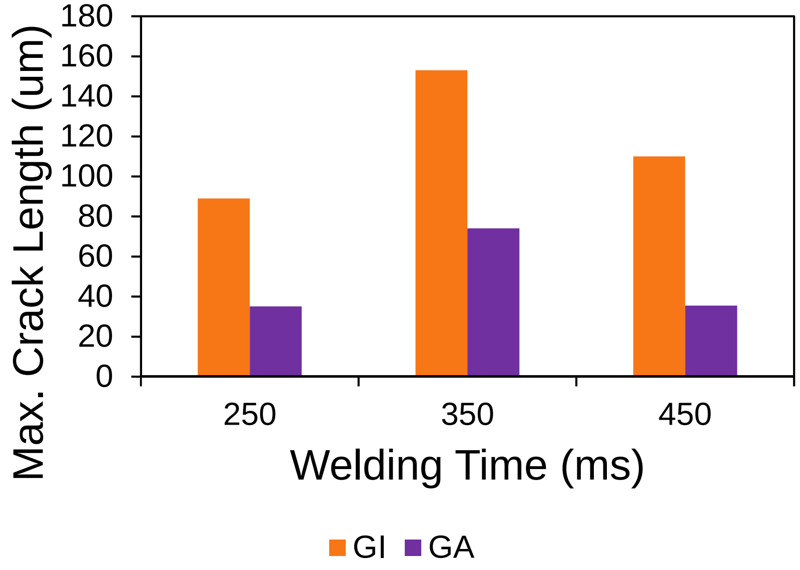

- In most cases, the GI coated samples displayed a longer maximum crack length than the GA coated samples welded with the same conditions

Welding Current and Time – MMnGI

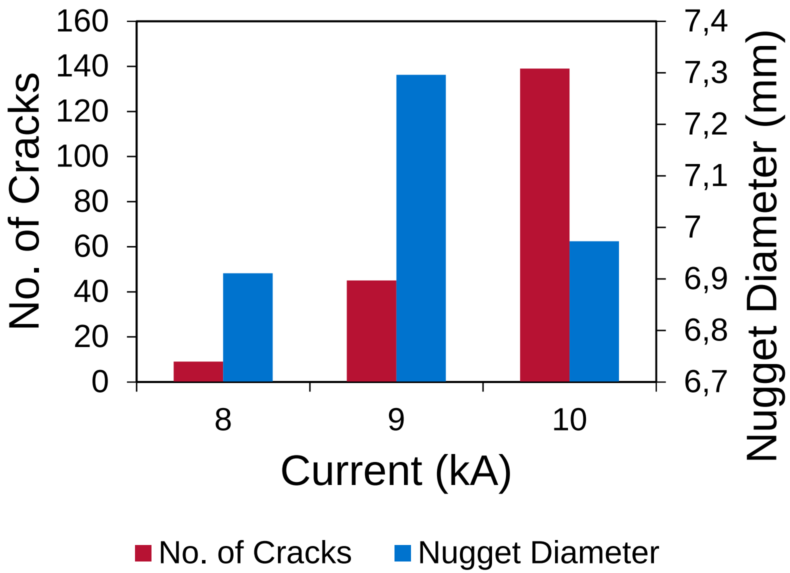

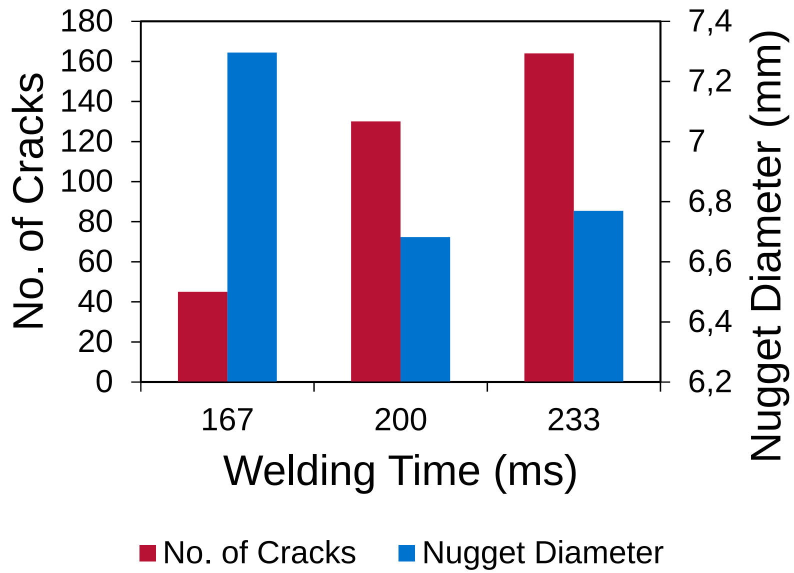

- Number of cracks increases with both increasing current and welding time
- Nugget diameter displays unexpected trends

Welding Current and Time – MMnGI

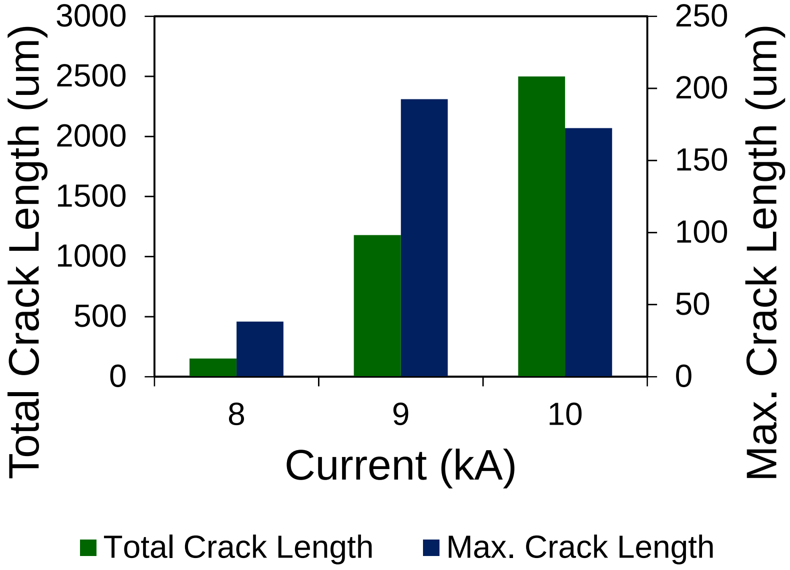

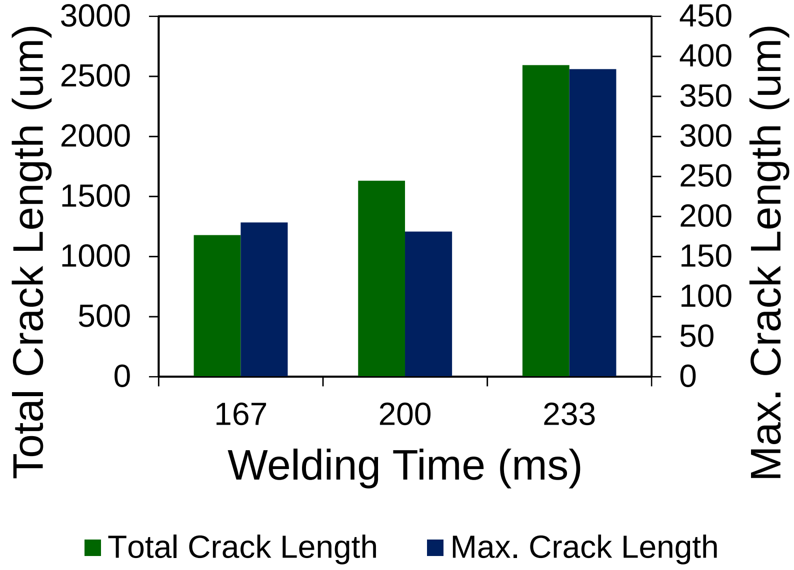

- Total crack length increases with both increasing current and weld time

Process Maps – MMnGI

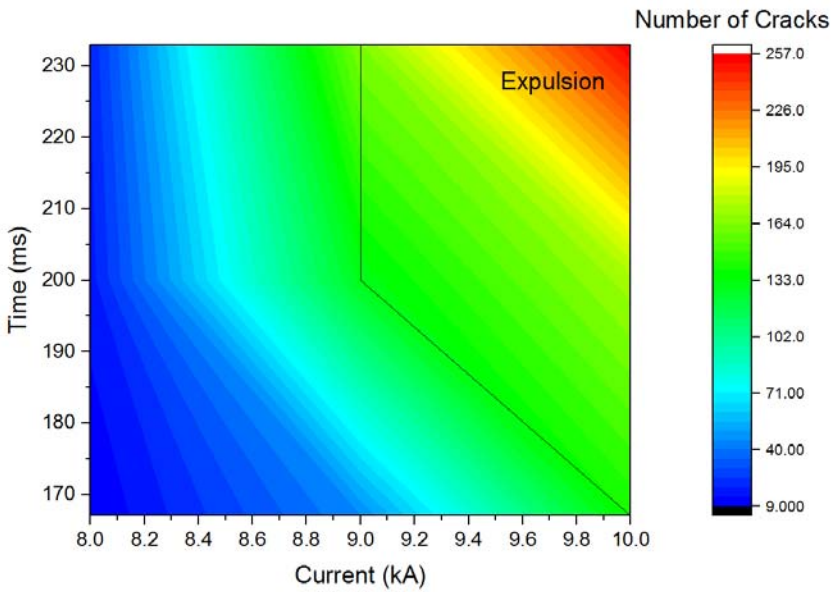

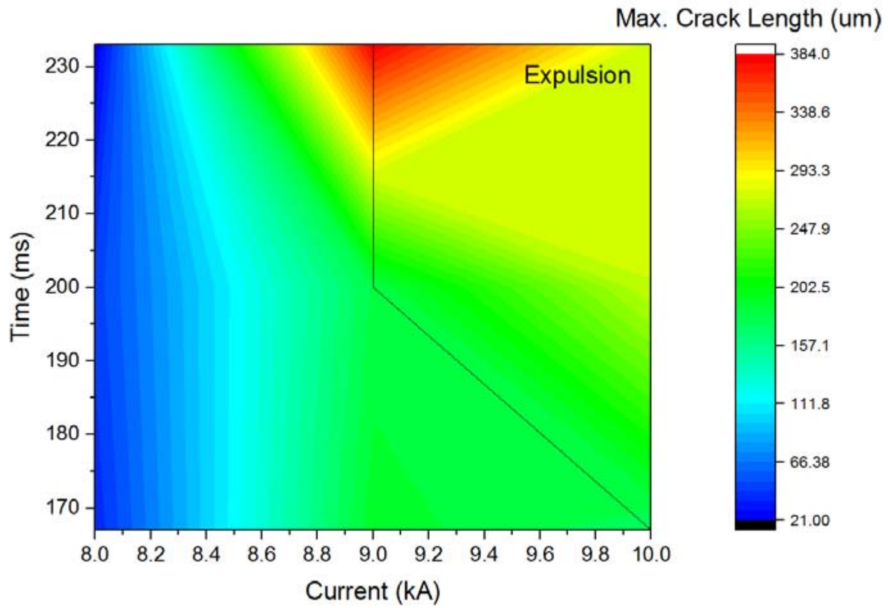

- Number of cracks shows the expected trend – highest cracking at highest current and time
- Maximum crack length shows a peak at 9 kA, 233 ms but otherwise shows expected trend

DP980GI vs MMnGI

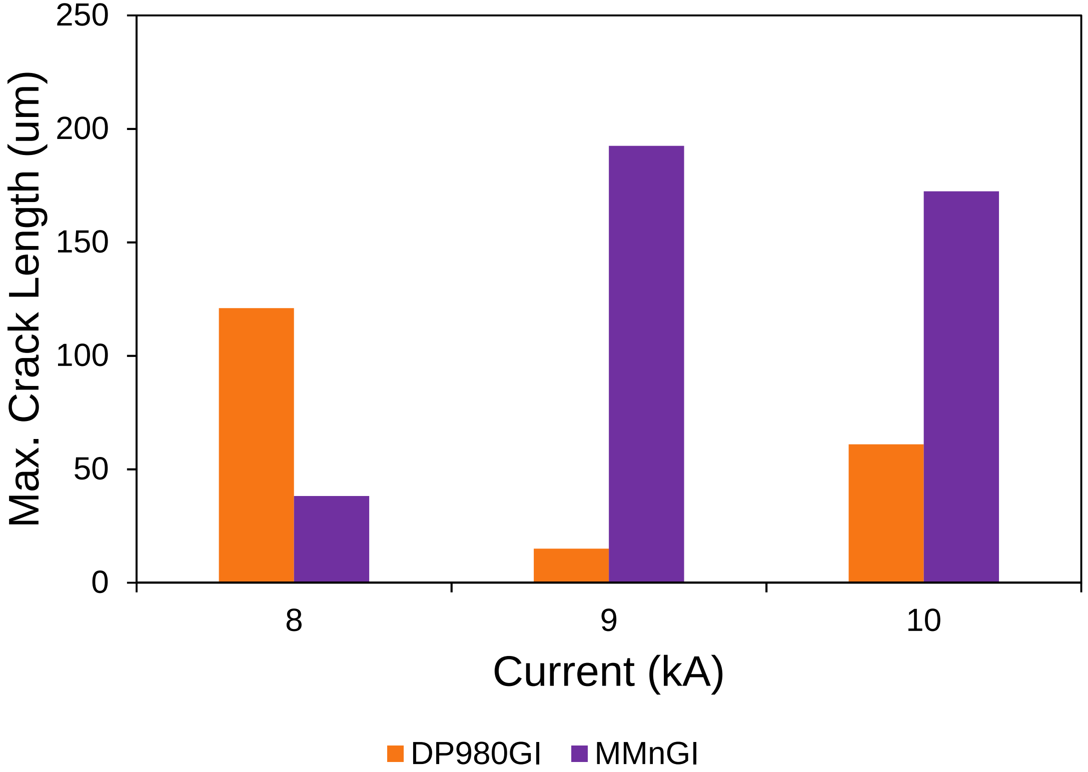

- In most cases, MMnGI (~50%RA) samples showed a greater maximum crack length than DP980GI(~1%RA) samples welded with the same current

UNIVERSITY OF WATERLOO

Gap Width (DP980GI)

- Single constrained

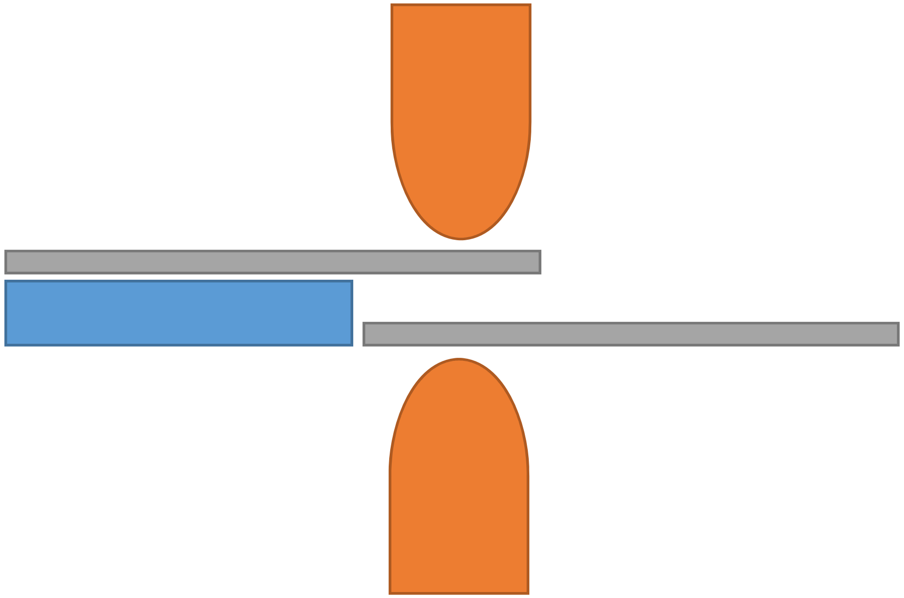

- Double constrained

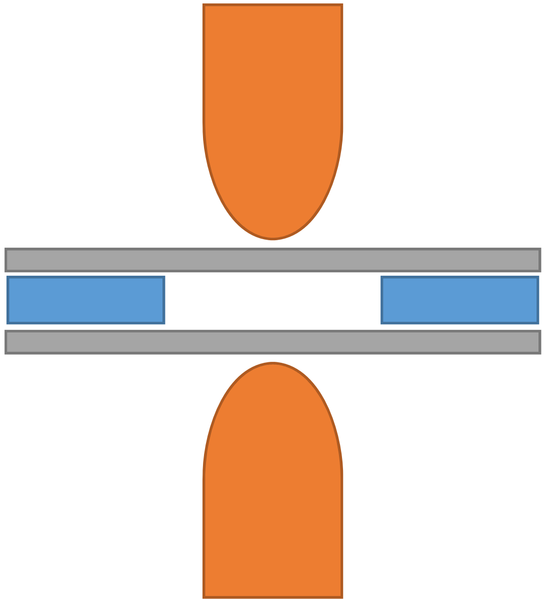

Gap Width (DP980GI)

- Single constrained

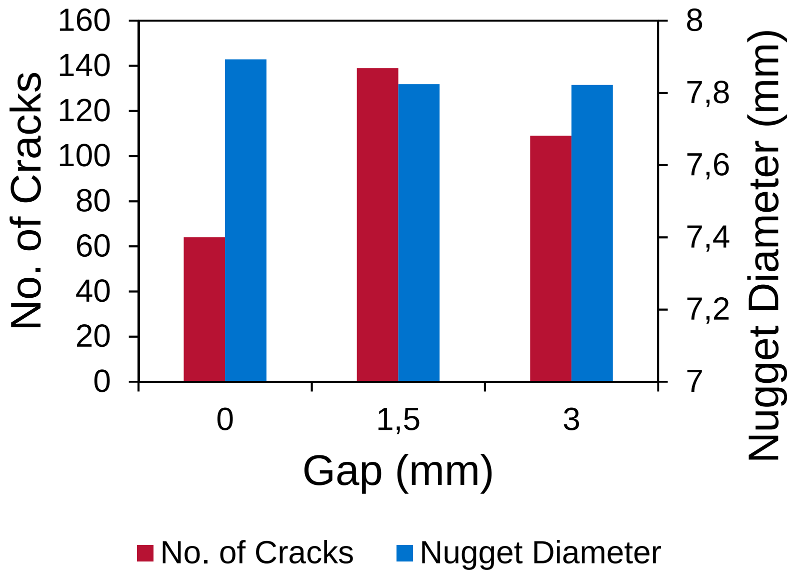

- Double constrained

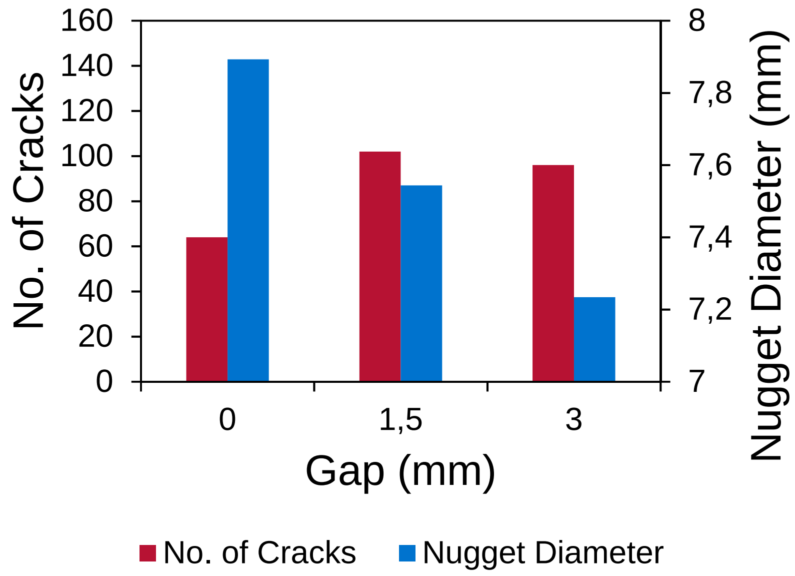

- Nugget diameter decreases with gap due to decreased contact area while number of cracks increases
- Both constraint conditions show a decrease in number of cracks between 1.5 and 3 mm gap, possibly because of the decrease in nugget diameter

Gap Width (DP980GI)

- Single constrained

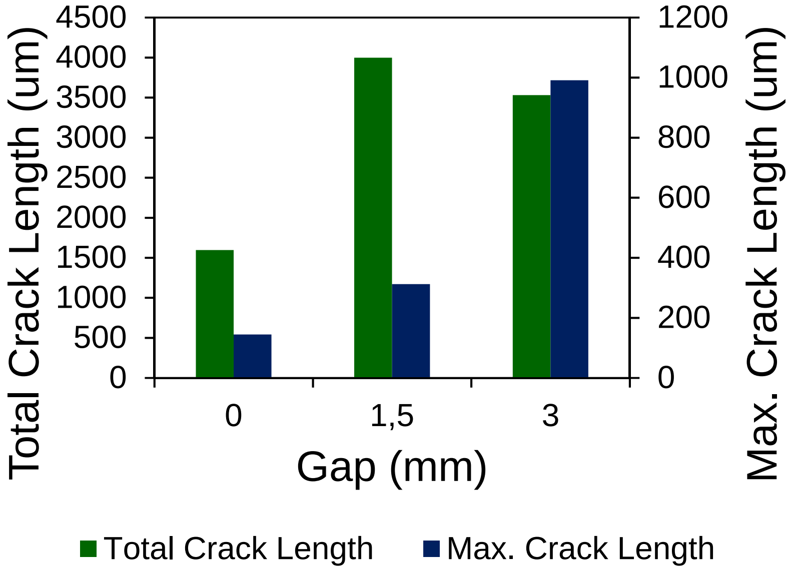

- Double constrained

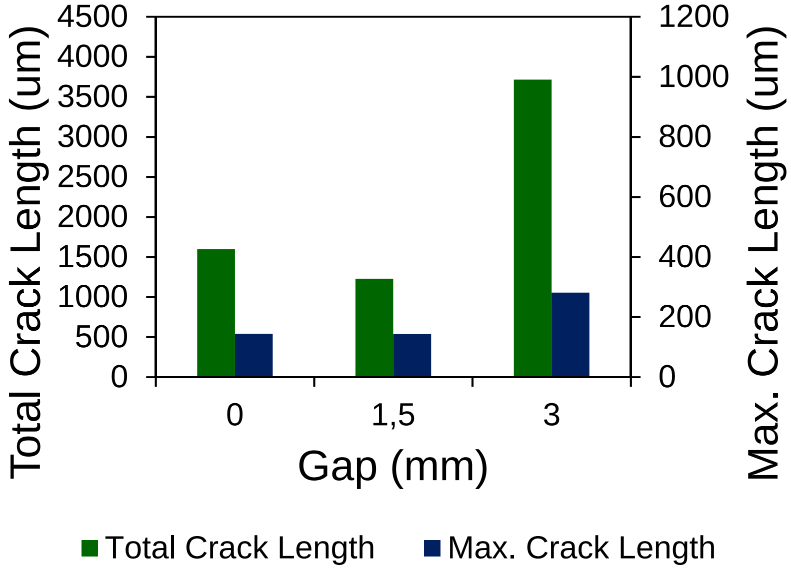

- Total and maximum crack lengths increased with increasing gap
- In general, single constrained condition showed longer crack lengths than double constrained due to larger nugget diameter

Pulse and Pre-current (DP980GI)

- Single pulse with pre-current

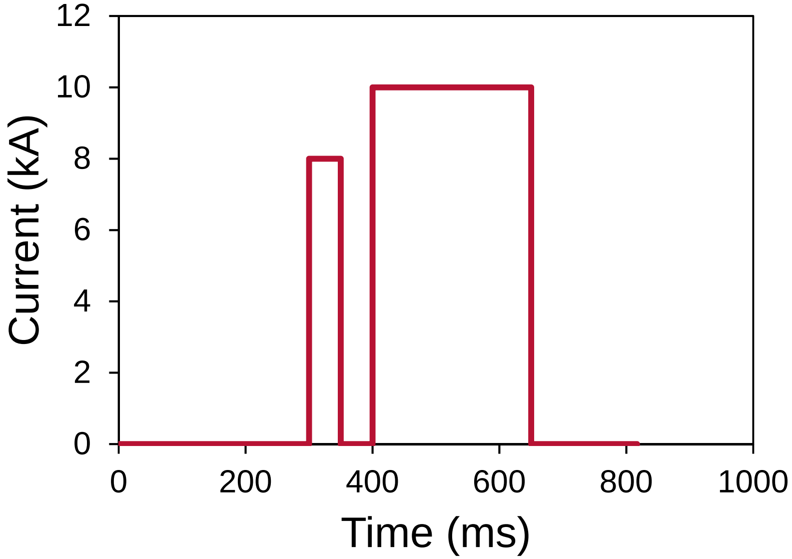

- Double pulse with pre-current

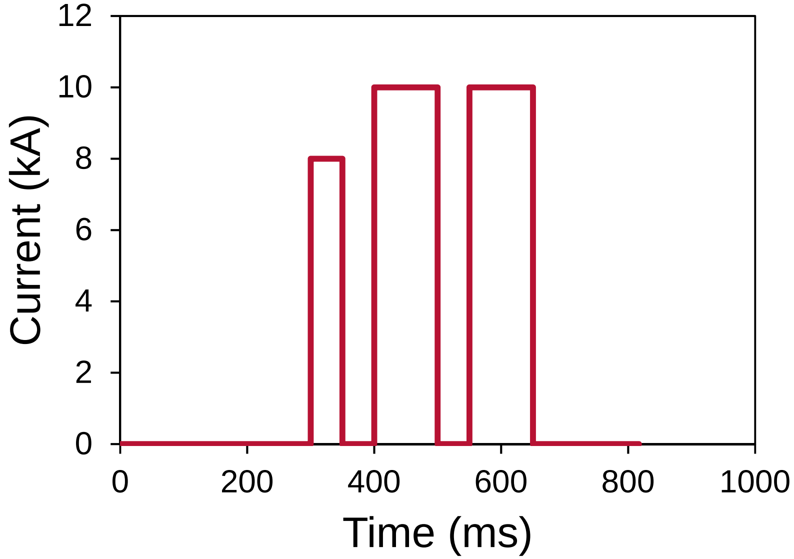

- Total welding time remains the same between the two conditions

Pulse and Pre-current (DP980GI)

10kA and 250ms

- Single pulse with pre-current

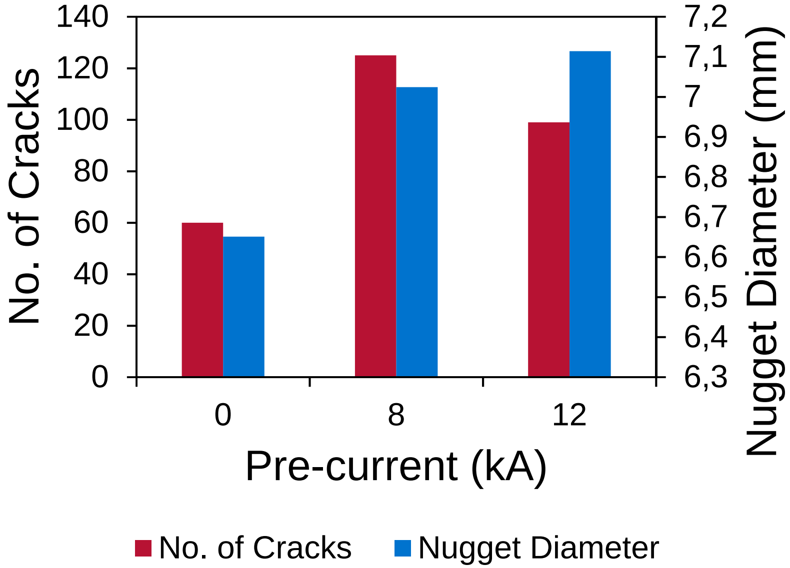

- Double pulse with pre-current

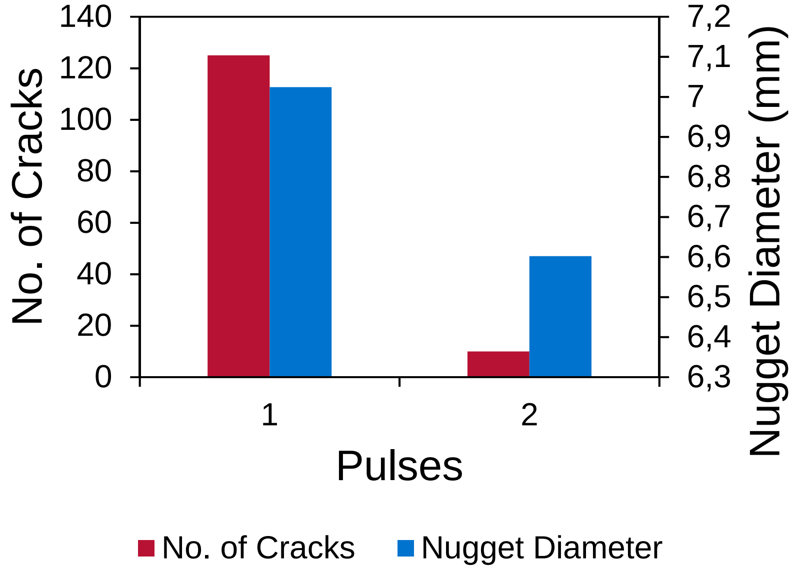

- Number of cracks increased with increasing pre-current due to increased nugget diameter
- Number of cracks decreased when welding with 2 shorter pulses due to a decrease in nugget diameter

Pulse and Pre-current (DP980GI)
10kA and 250ms

- Single pulse with pre-current

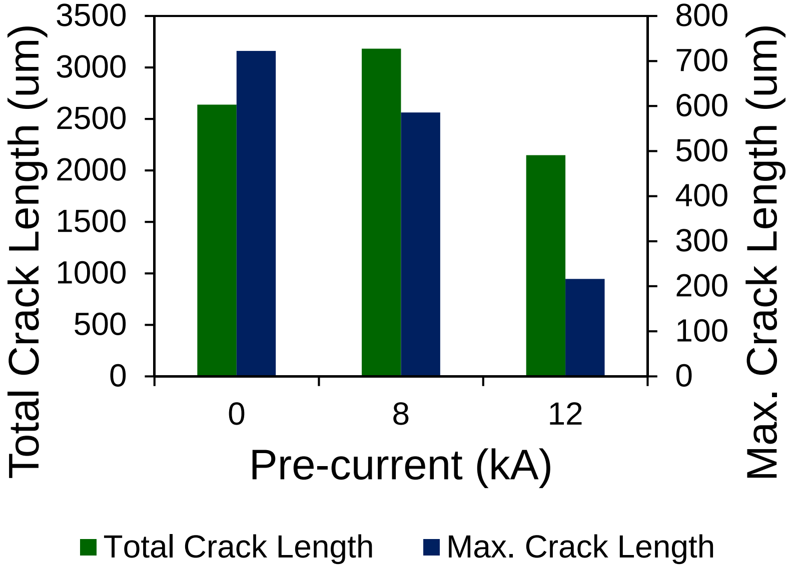

- Double pulse with pre-current

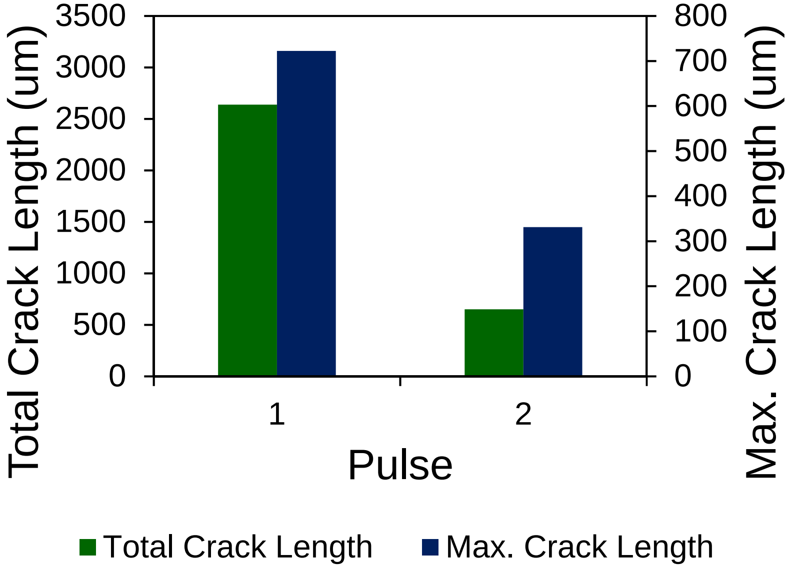

- Total and maximum crack lengths decreased with increasing pre-current
- Total and maximum crack lengths decreased when welding with 2 shorter pulses

Stackup (MMnGI)

- 2-Stack

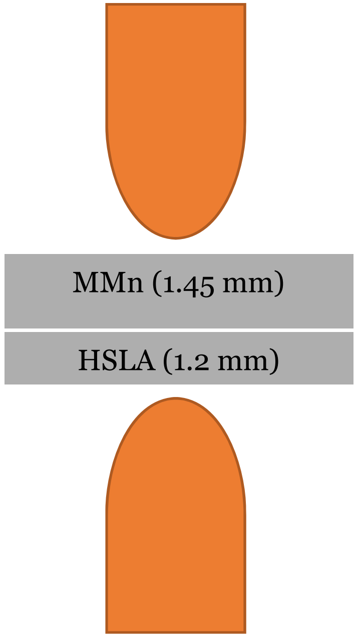

- 3-Stack

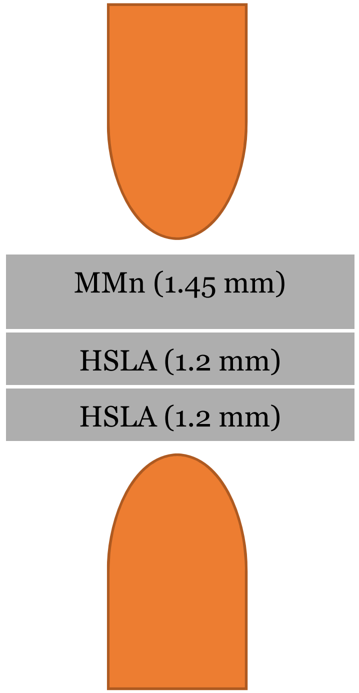

Stackup (MMnGI)

- 2-Stack

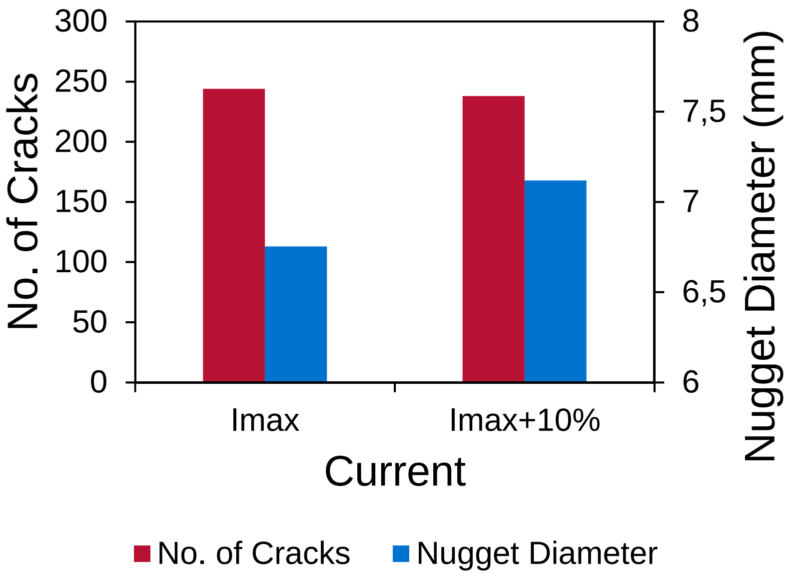

- 3-Stack

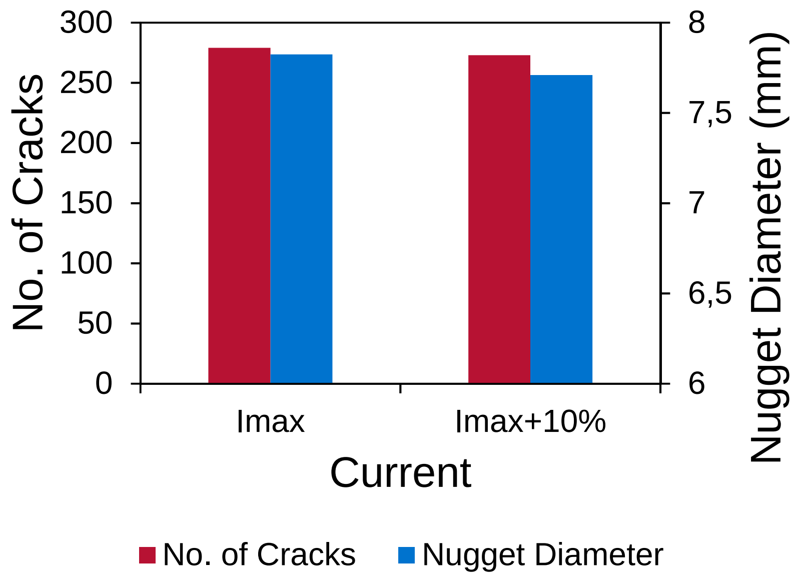

- Nugget diameter increased with increasing current for 2-stack condition but remained relatively constant for 3-stack condition
- Both stackup conditions show little change in number of cracks with changing current

Stackup (MMnGI)

- 2-Stack

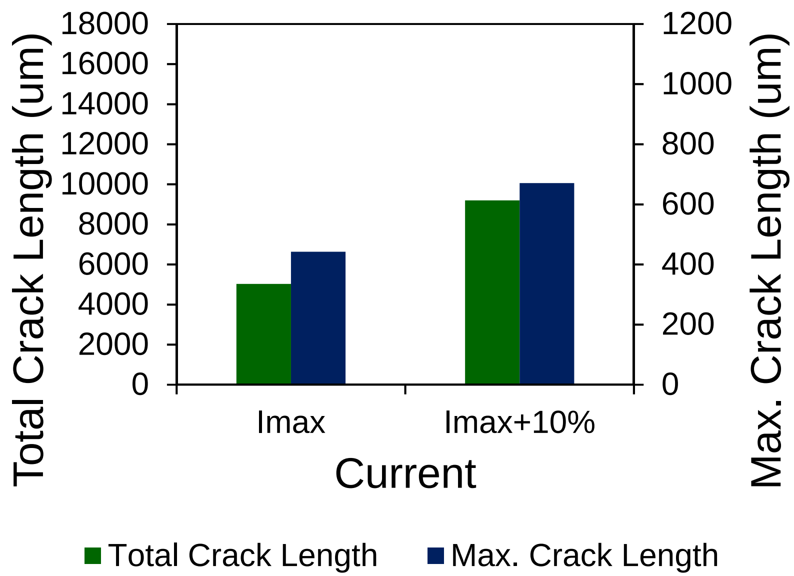

- 3-Stack

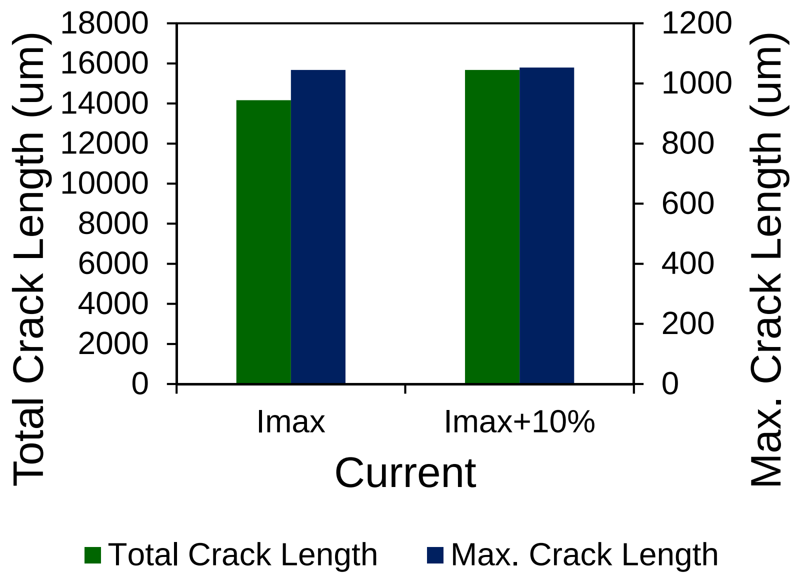

- Longer total and maximum crack lengths observed in 3-stack condition than 2-stack
- Very little difference in total and maximum crack length between current conditions in 3-stack

Crack Location

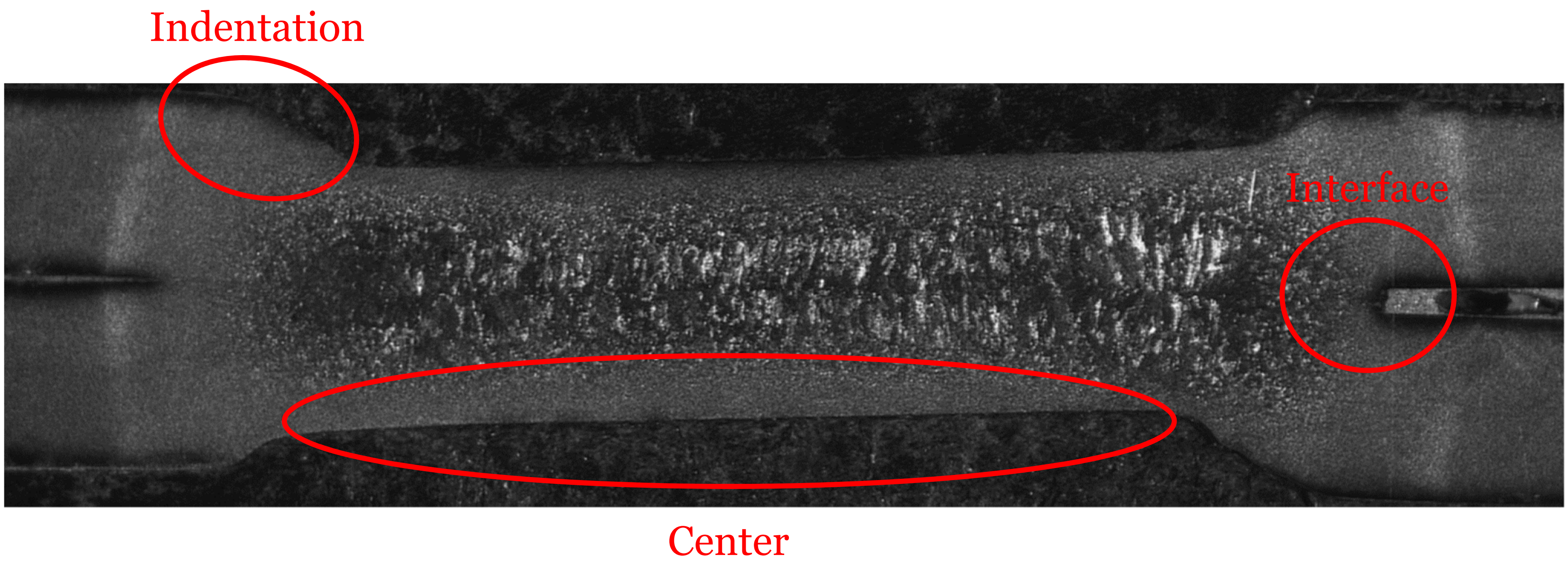

UNIVERSITY OF WATERLOO

Crack Location (DP980GI)

- Indentation Cracks

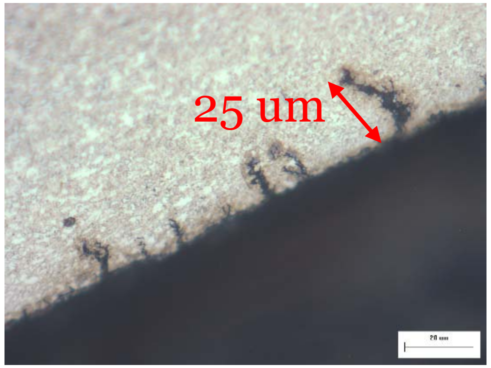

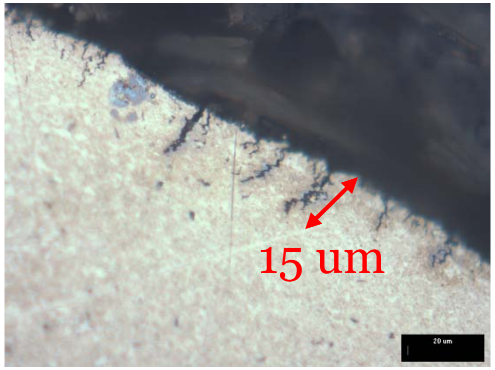

- Center Cracks

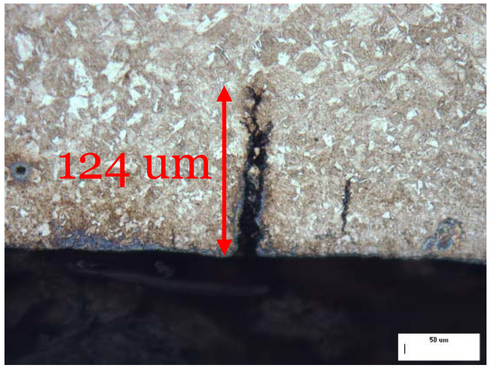

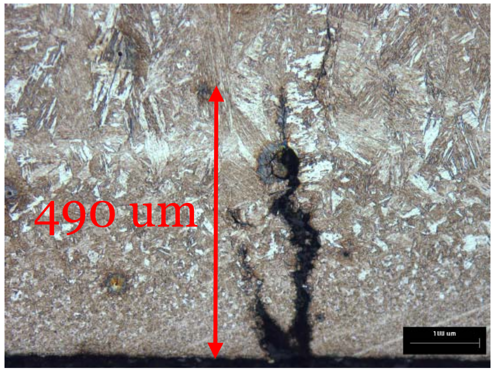

10 kA, 450 ms

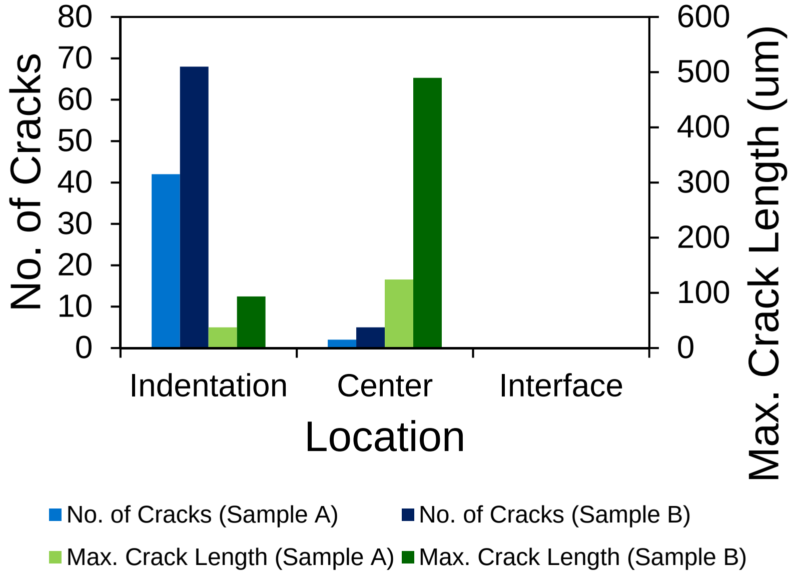

- More cracks in indentation but longer cracks in center
- Cracks rarely observed in interface

Crack Location (MMnGI)

- Indentation Cracks

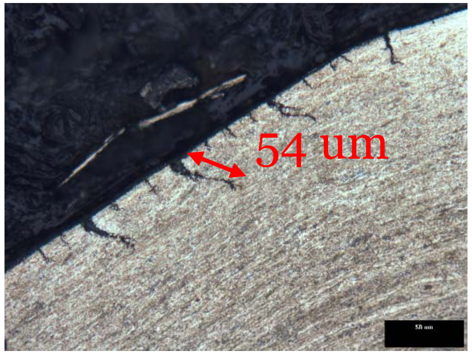

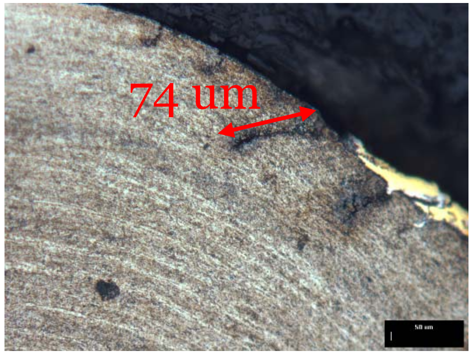

- Center Cracks

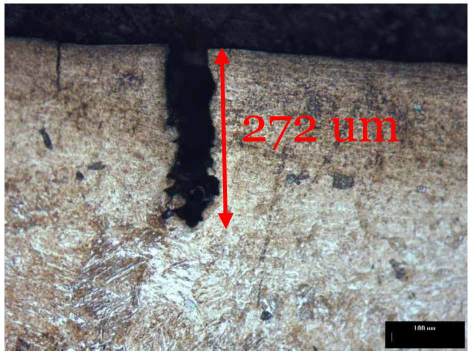

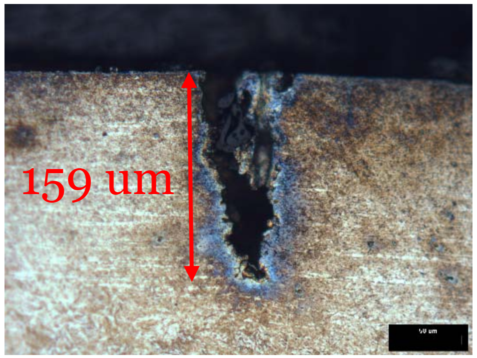

10 kA, 233 ms

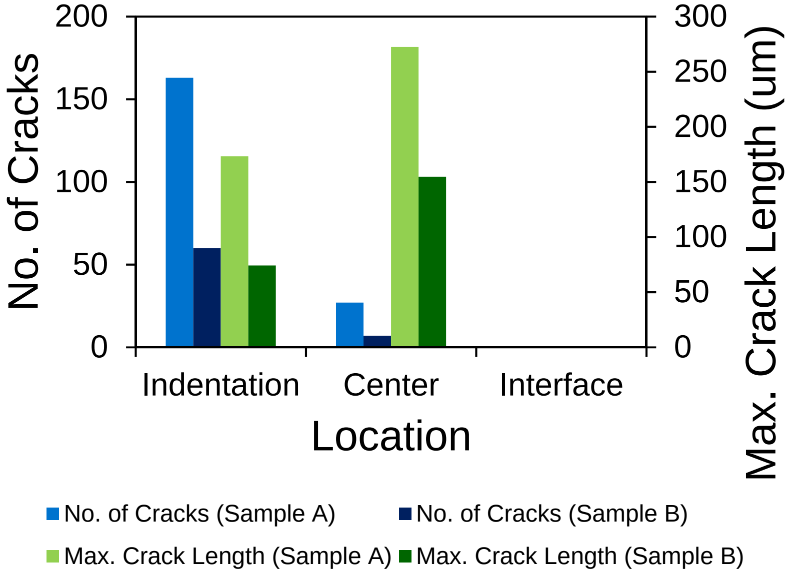

- More cracks in indentation but longer cracks in center
- Cracks rarely observed in interface

UNIVERSITY OF WATERLOO

Summary - RSW

- Increasing current and welding time increases extent of cracking.
- DP980GI steel is more susceptible to LME than DP980GA.
- MMnGI (~50%RA) is more susceptible to LME than DP980GI (~1%RA).
- Welding with gap increases the amount of cracking and decreases the nugget diameter.
- Welding with pre-current increases nugget diameter, increases number of cracks and decreases maximum crack length.
- Welding with two short pulses decreases nugget diameter and amount of cracking.
- 3-stacks are more susceptible to LME than 2-stacks.
- A larger number of cracks are observed in indentation than center, but center cracks tend to be longer.

Fiber laser welding

Fiber Laser Welding of 22MnB5 (GA-coated)

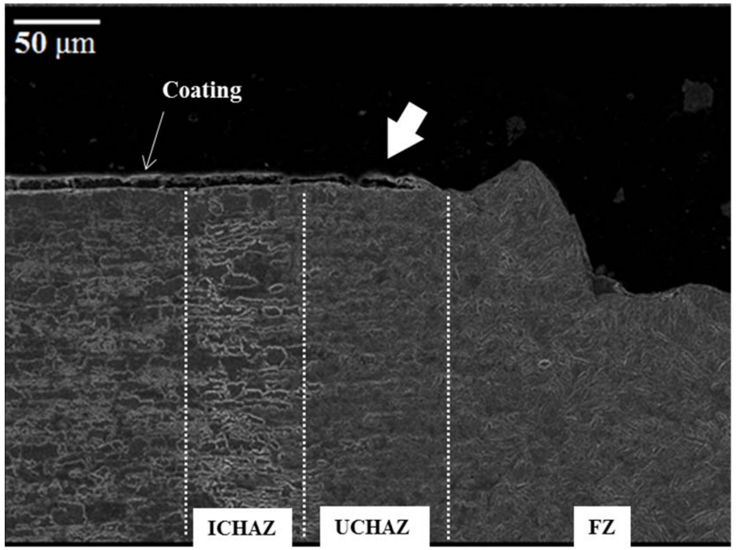

- **UCHAZ**

$$Ac_3(\,^{o}C) = 937 - 476C - 19.7Mn - 16.3Cu - 26.6Ni - 4.9Cr + 56Si + 38.1Mo + 12.5V - 19Nb + 198Al + 3315B$$

➡ **T>845°C**

Formation of austenite in UCHAZ plus melting point of GA-coating

➡ **Chance of LME in the presence of tensile loads**

UNIVERSITY OF WATERLOO

Introduction

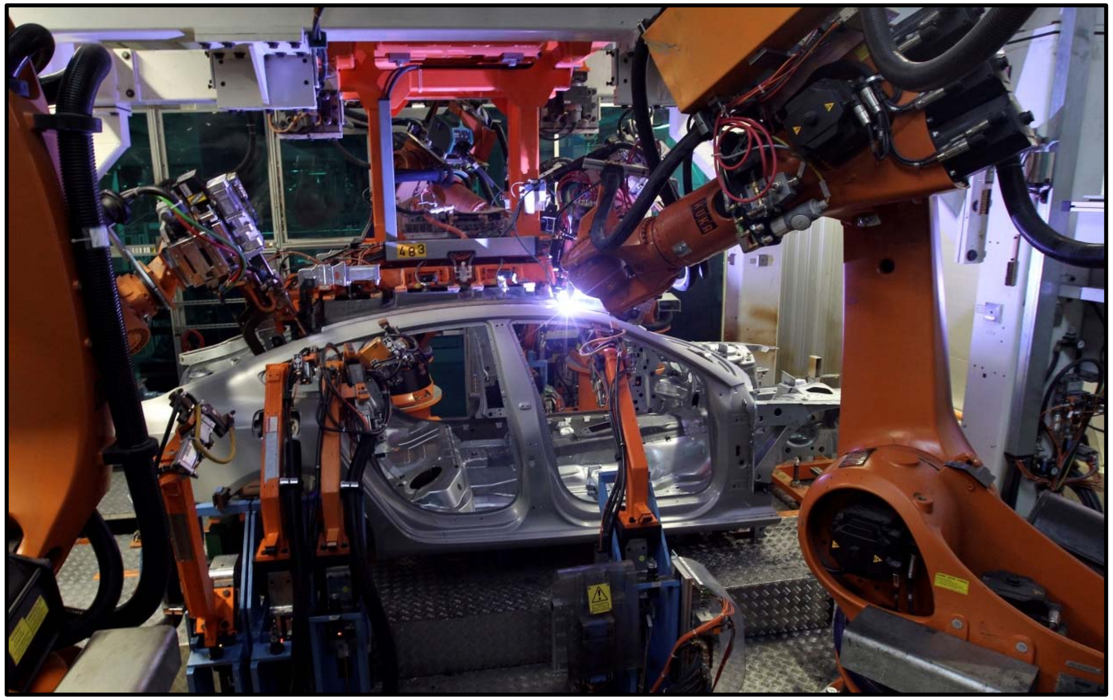

LBW Assembly of the body-in-white

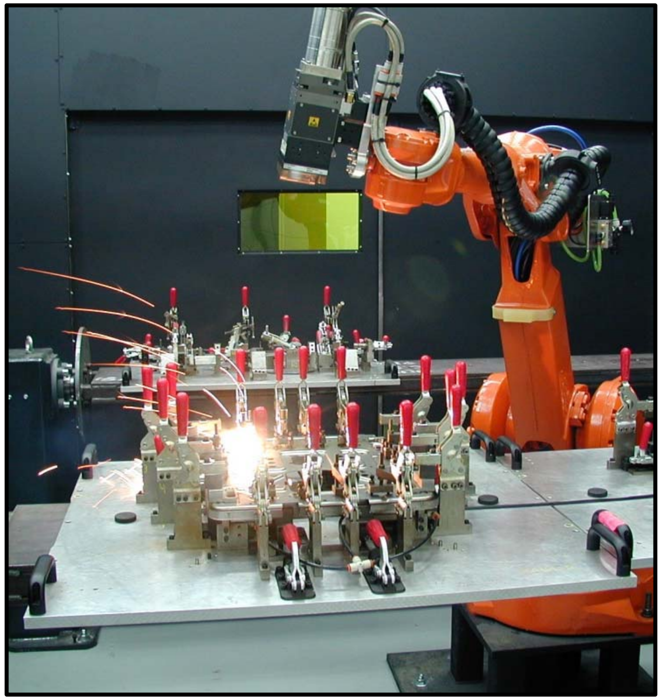

TWB Production

Susceptible Microstructures (Austenitic)

The Liquid Metal (Zn)

The Presence of Tensile Stresses

Restrained LBW

Grain Boundary Decohesion

The rapid intergranular propagation of LME-cracks

Developed Setup

➢ Apply External loading

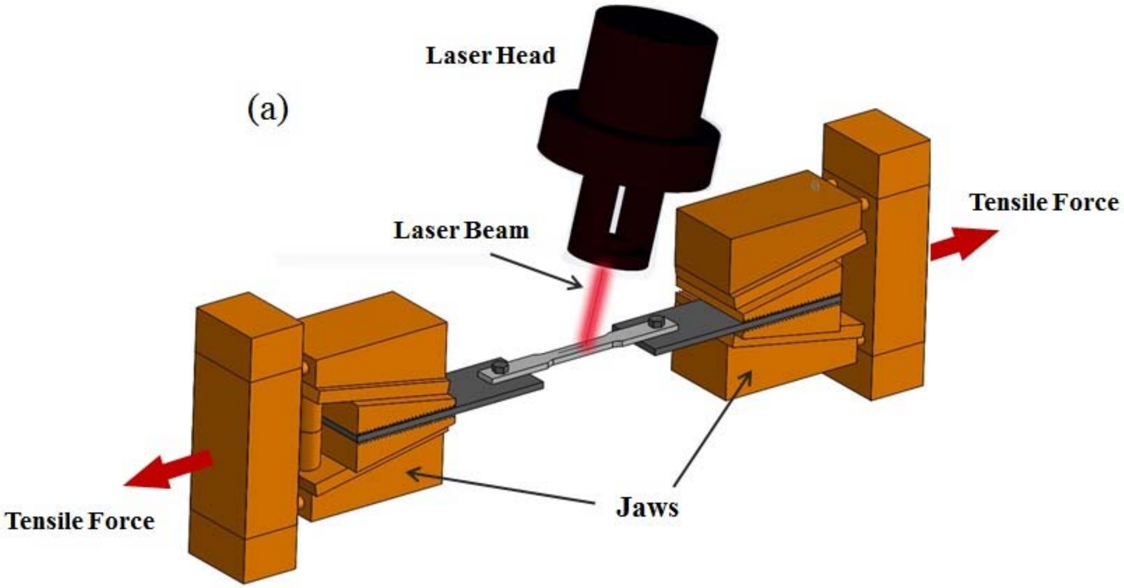

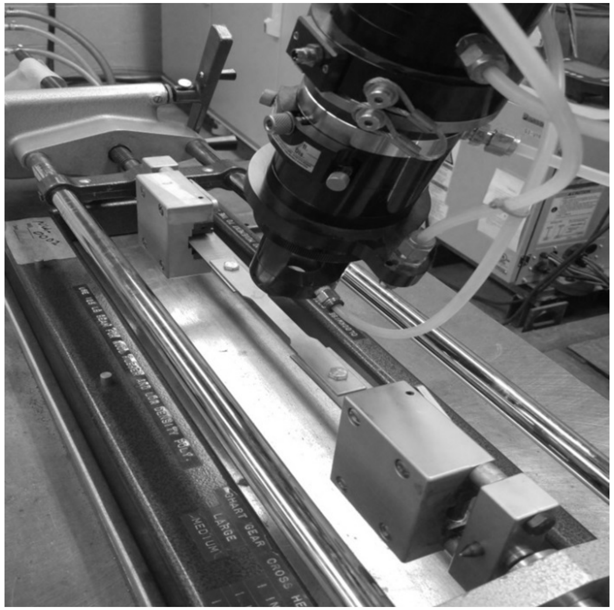

Results

- 22MnB5 Press-Hardening Steel GA-coated

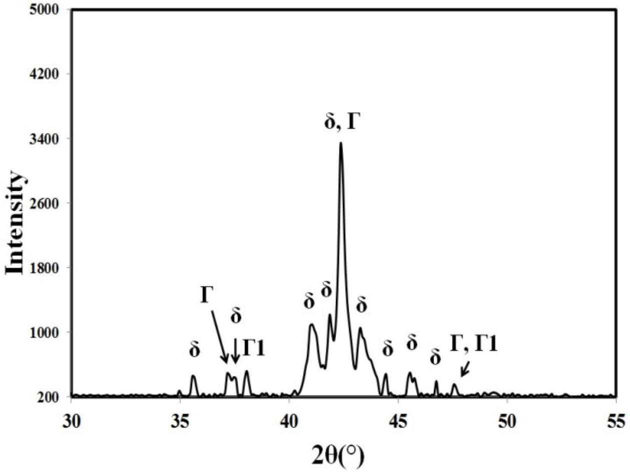

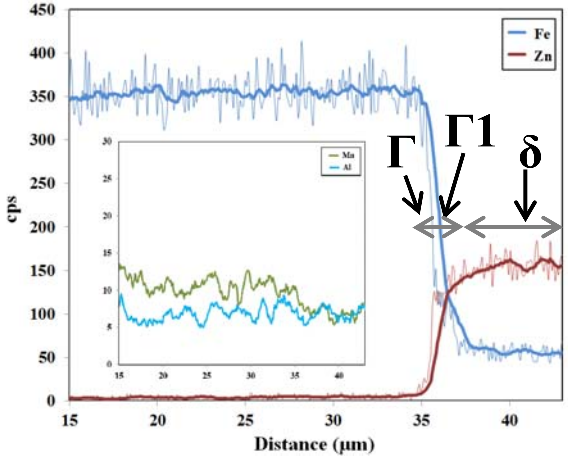

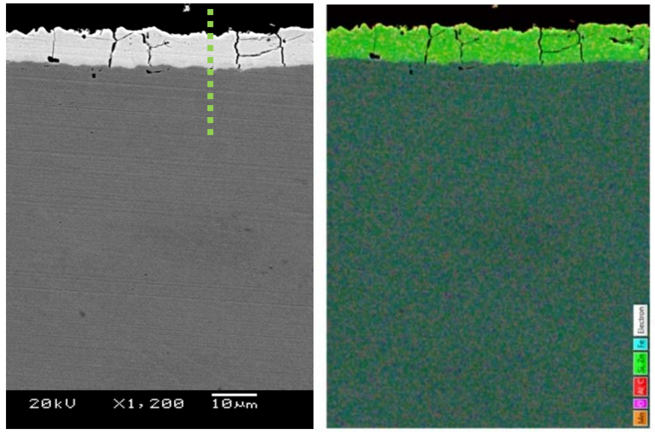

UCHAZ

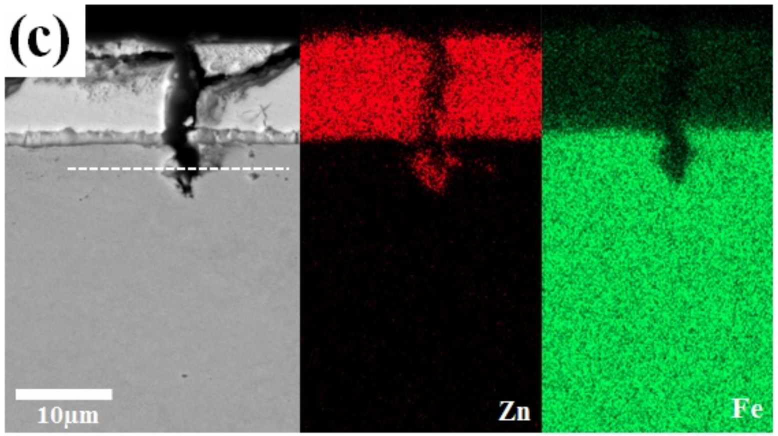

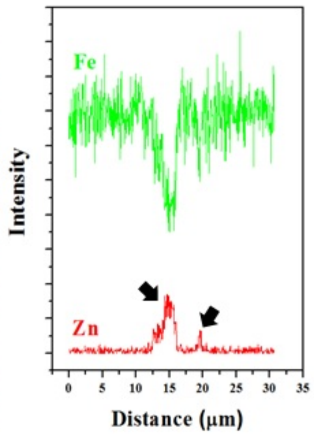

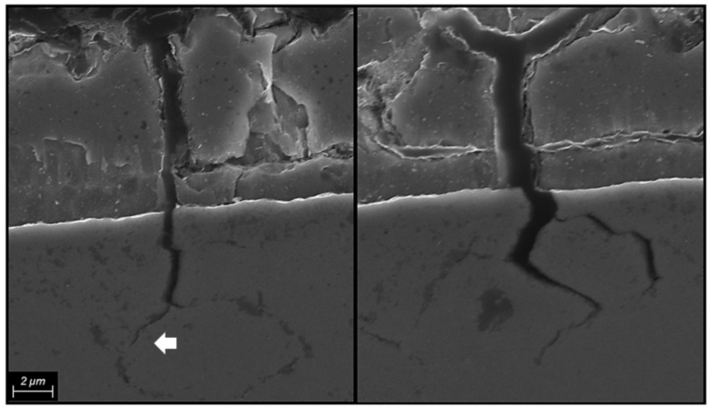

UNIVERSITY OF WATERLOO

Results

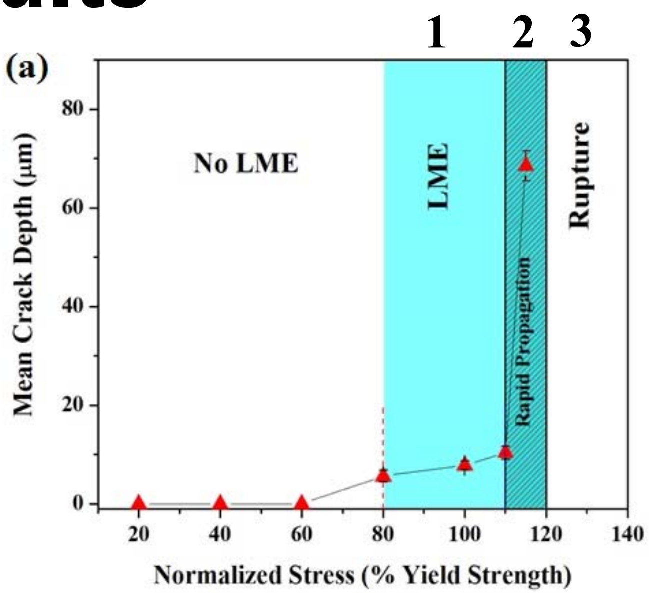

1
2
3
(a)
No LME
LME
Rapid Propagation
Rupture
Mean Crack Depth (µm)
0
20
40
60
80
20
40
60
80
100
120
140
Normalized Stress (% Yield Strength)

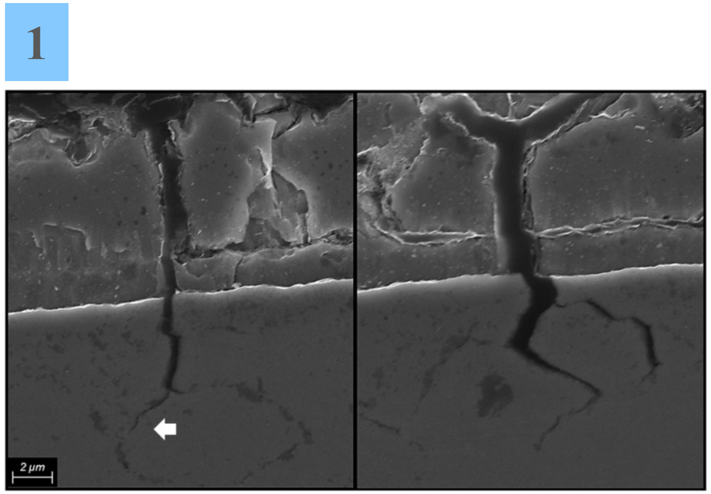

1
2 µm

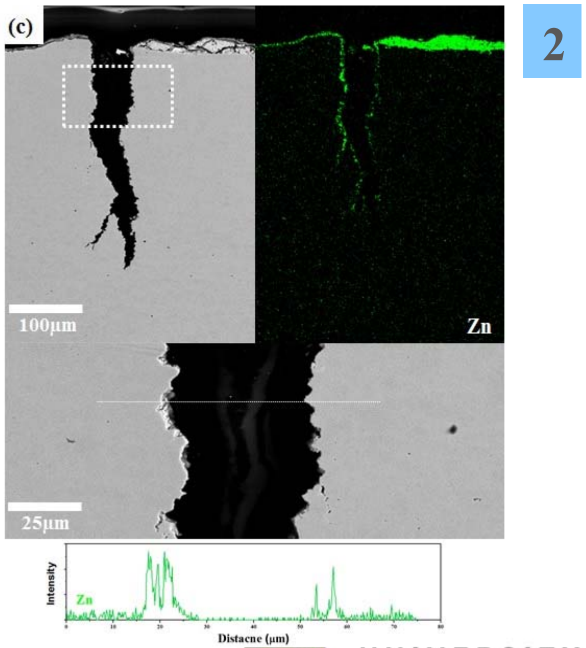

(c)
2
100µm
Zn
25µm
Intensity
Zn
Distacne (µm)

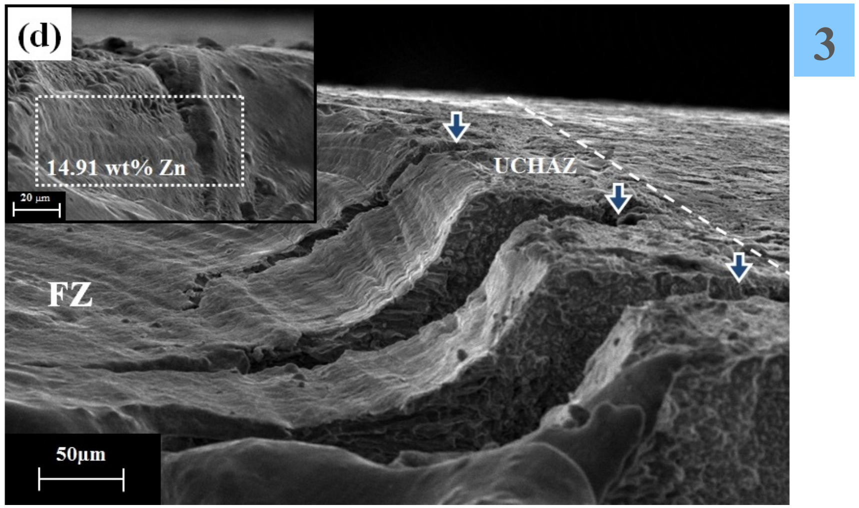

(d)
3
14.91 wt% Zn
20 µm
UCHAZ
FZ
50µm

Mechanism

Liquid-Metal-Induced Embrittlement (LMIE)

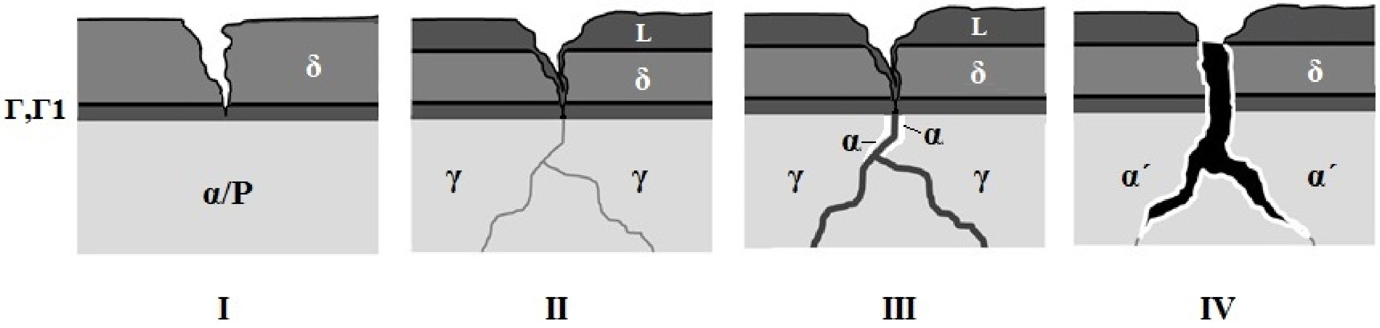

The embrittling mechanism was caused **not** directly by the Zn-liquid

Zn is a **strong ferrite stabilizing solute** in Fe

Partial transformation of γ-Fe to α-Fe(Zn)

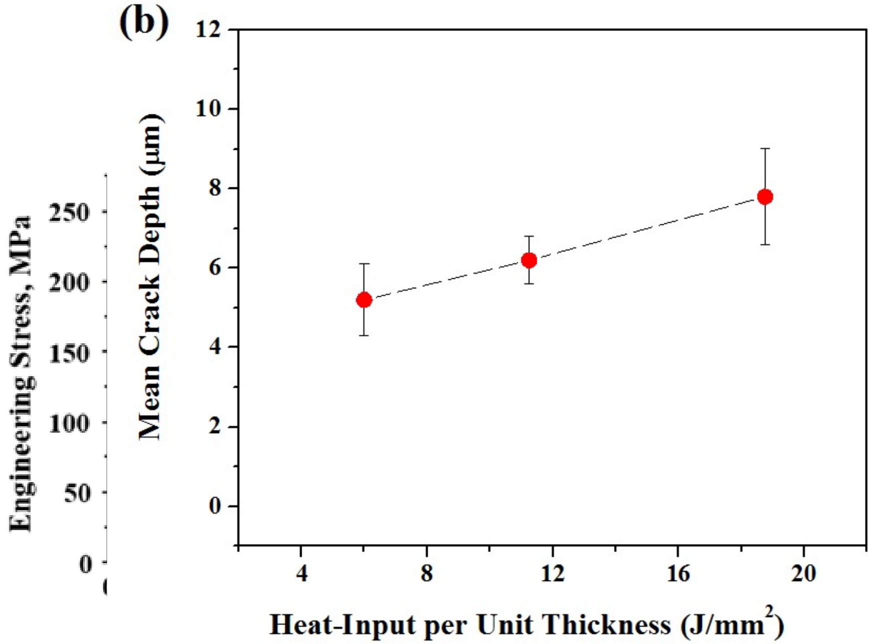

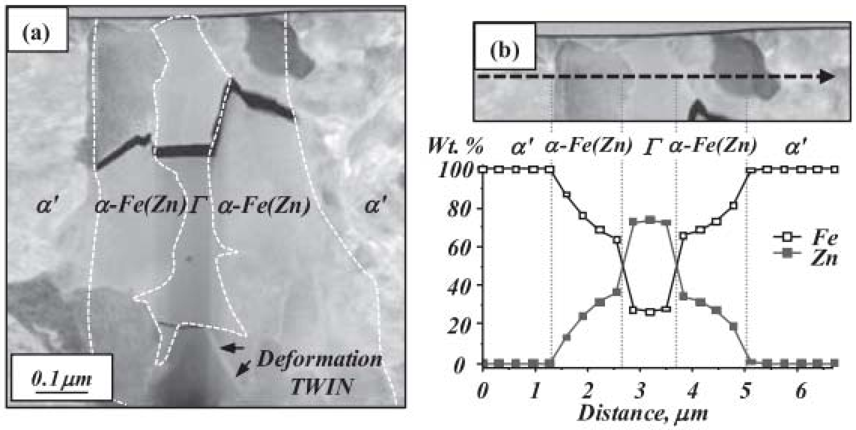

UNIVERSITY OF WATERLOO

❑ H. Kang, L. Cho, C. Lee, B.C. De Cooman, Metall. Mater. Trans. A Phys. Metall. Mater. Sci. 47 (2016) 2885–2905.

Results

- Restrained Dissimilar Lap Joining
- TWIP steel — Not-coated
- Mid-Mn TRIP steel — GI-coated

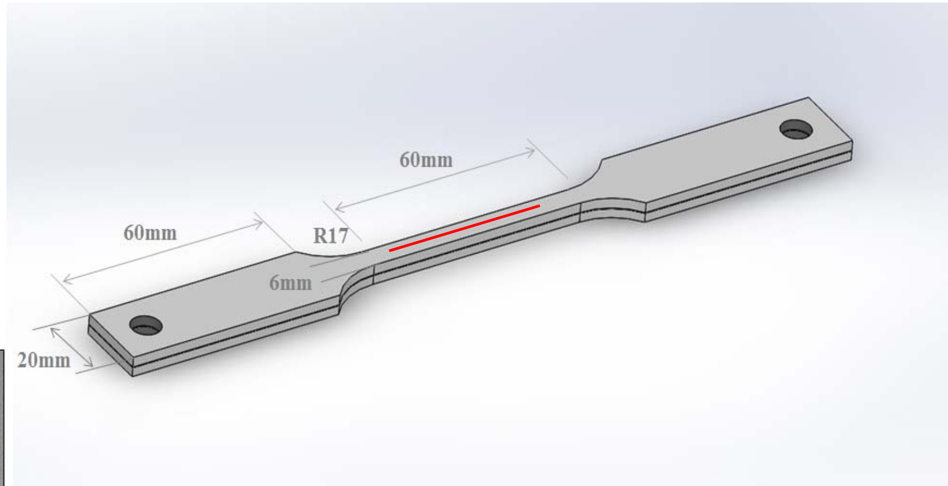

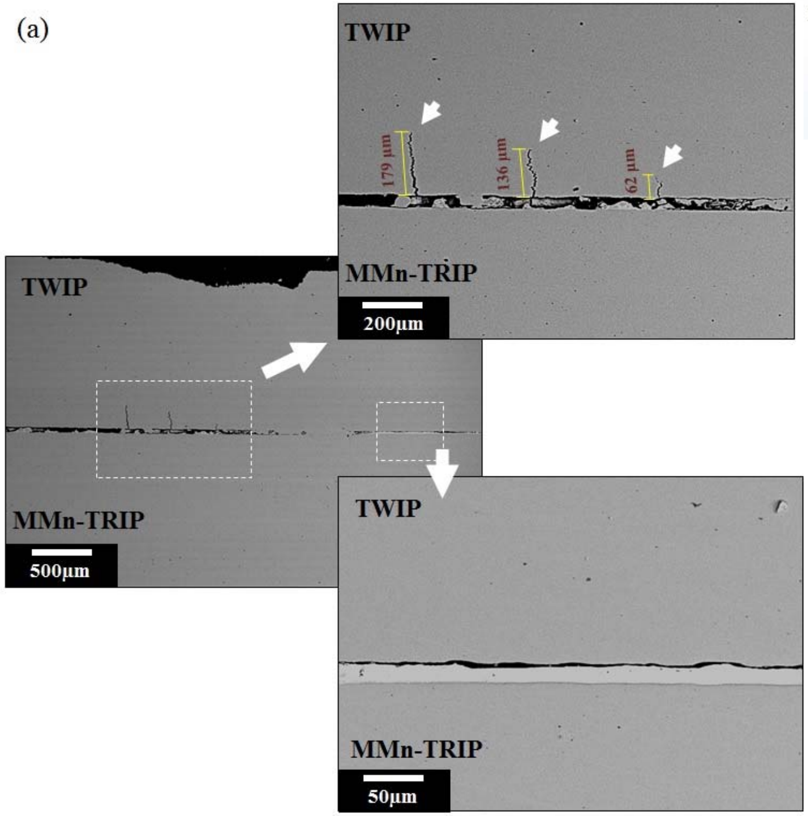

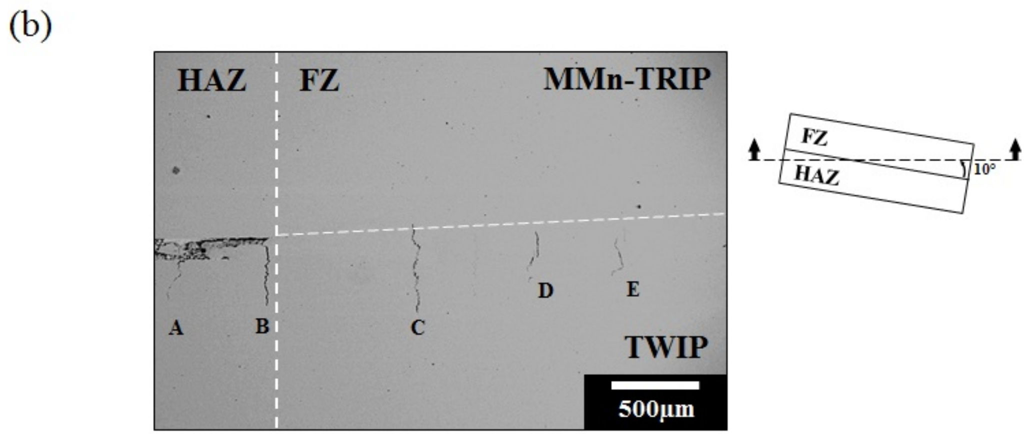

UNIVERSITY OF WATERLOO

Results

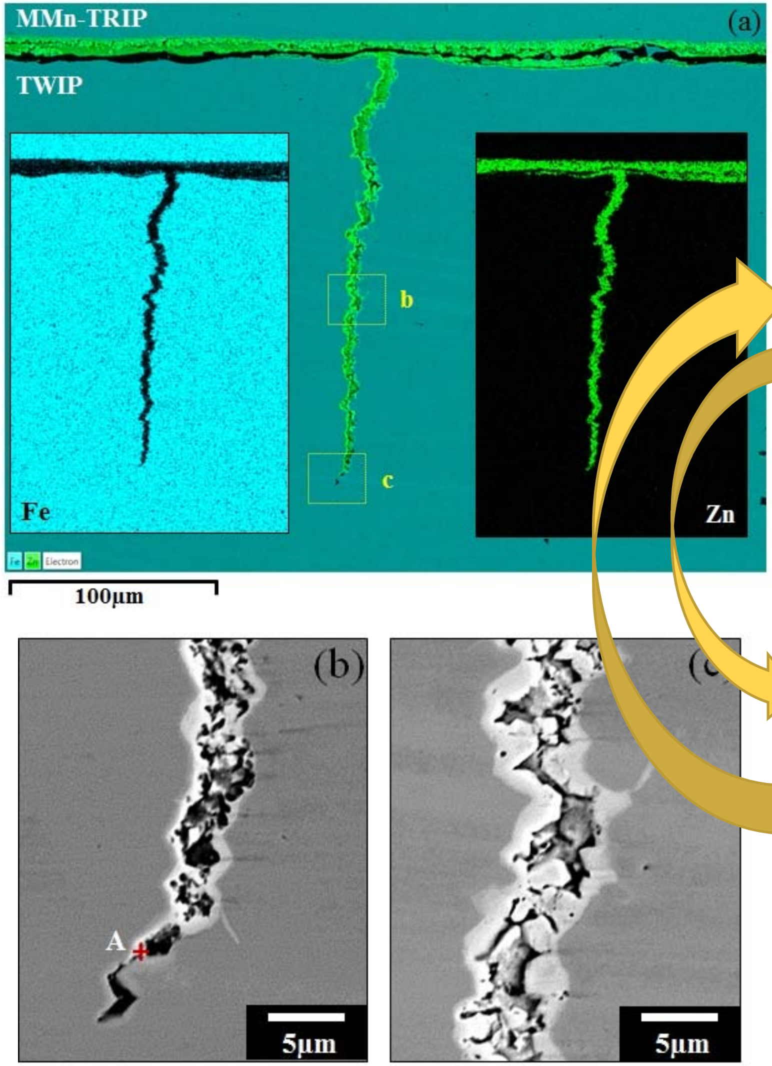

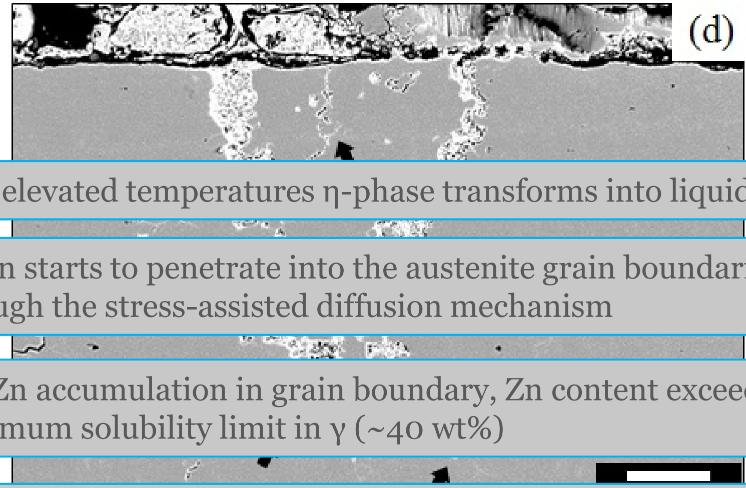

I. At elevated temperatures η-phase transforms into liquid phase

II. Zn starts to penetrate into the austenite grain boundaries through the stress-assisted diffusion mechanism

III. Zn accumulation in grain boundary, Zn content exceeds the maximum solubility limit in γ (~40 wt%)

IV. Over the maximum solubility limit, liquid-Zn starts to form along the austenite grain boundaries

V. As a consequence of liquid-Zn film along grain boundaries, the metallic bond weakening takes place **crack opens up**

by the crack opening, more liquid-Zn from the melted coating flow into the crack through the **capillarity effect**

Point B: 71.2 wt% of Zn, 5.8 wt% of Mn and 0.9 wt% of

during LBW cooling cycle, the present liquid phase inside the crack and the austenite matrix transform into Γ-(Fe,Mn)$_3$Zn$_{10}$ phase through the **peritectic reaction**

γ(Fe, Mn, Zn)+Liq. Zn (Fe, Mn-saturated)→ Γ-(Fe, Mn)$_3$Zn$_{10}$

Results

Stress-Assisted Diffusion Mechanism

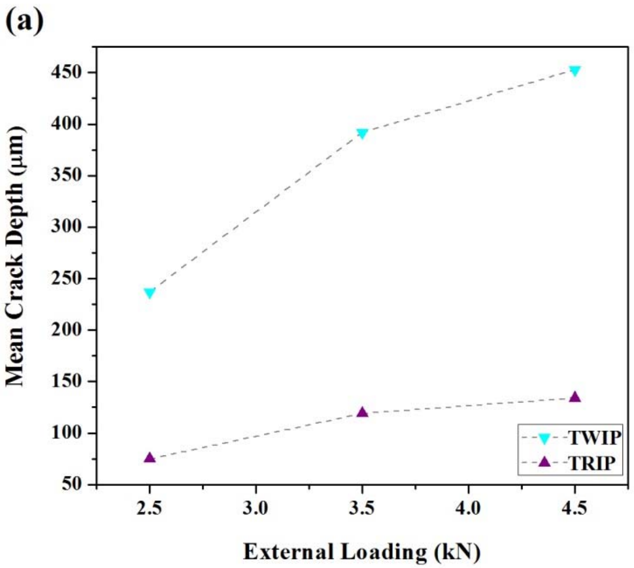

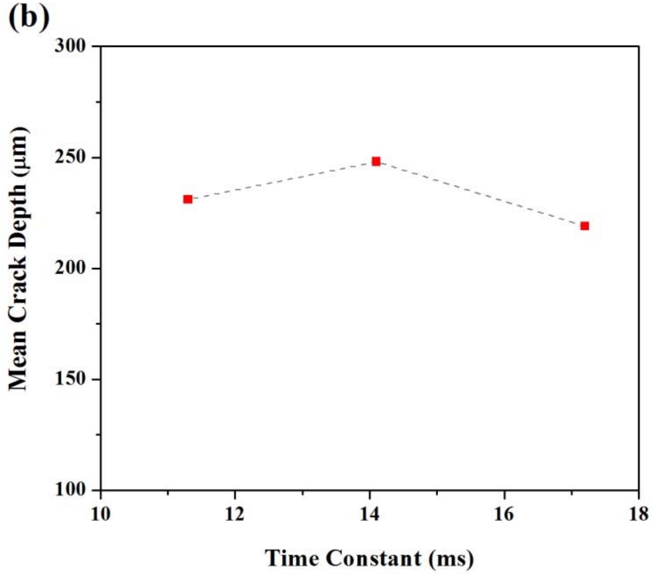

- Rosenthal model

$$\tau = \frac{1}{4\pi e\lambda\rho c}\frac{\left[\frac{Q_{net}}{vd}\right]^2}{\left(T_{Ac_1} - T_0\right)^2}$$

$$\frac{Q_{net}}{vd} = \frac{\rho c(r_{Ac_1} - r_m)(2\pi e)^{1/2}}{\left(\frac{1}{T_{Ac_1} - T_0} - \frac{1}{T_m - T_0}\right)}$$

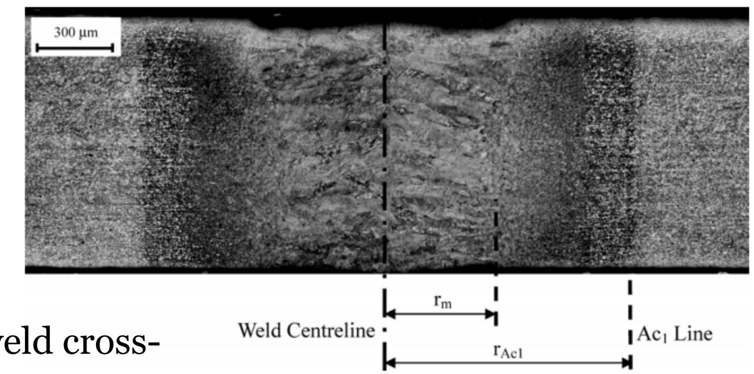

r_{Ac_1} and r_m are the isotherm positions of T_{Ac_1} and T_0 from the weld cross-sections

- M.F. Ashby, K.E. Easterling, Acta Metall. 30 (1982) 1969–1978.

Summary – Laser welding

- SEM/EDS results revealed the susceptibility of LMIE during Fiber Laser Welding of GA-coated 22MnB5 PHS under restrain condition.
- Mechanism: Partial transformation of δ-phase into liquid phase in UCHAZ, and penetration into the characteristic coating cracks and subsequent formation of α-Fe(Zn) along austenite grain boundaries
- The LME-cracking during restrained laser lap joining of high-Manganese TWIP and medium-manganese TRIP steel
- EDS analysis approved the presence of Γ-$(Fe,Mn)_3Zn_{10}$ phase inside the cracks, showing the penetration of liquid zinc during LBW
- Mechanism: The stress-assisted diffusion of Zn into the austenite grain boundaries and further liquid-Zn formation by a peritectic reaction

Project Status-ZCO-80

	Milestones / Period	Apr – Jun 2017	Jul – Nov 2017	Dec 2017 – May 2018	Jun 2018 – Mar 2019	Apr – Aug 2019	Sept 2019 – Mar 2020
1	Procurement of GI and GA coated AHSS Steel						
2	Effect of process parameters and welding conditions						
3	Thermomechanical simulation of various coatings on AHSS steels						
4	Evaluate the effect of various microstructural attributes						
5	Numerical Model to predict stress field present during welding						
6	Correlate the mechanical properties to the onset of LME						
7	ZCO-73 project final report						

UNIVERSITY OF WATERLOO

Future Work

- LME susceptibility analysis for new TRIP steel
- Gleeble Testing for all material and coating conditions
- Welding with external load (RSW)
- Continue testing with gap and pulse/pre-current
- Experimenting with stack-up conditions

Materials we need

- TWIP steel with GA or GI or EG coated

UNIVERSITY OF WATERLOO

Acknowledgements

- Frank Goodwin, **International Zinc Association**
- Elliot Biro, **ArcelorMittal Dofasco**
- **Baosteel** for providing material

Thank You!

Further Questions – Contact:

Professor Norman Zhou
University of Waterloo
200 University Ave. W.
Waterloo, ON, N2L 3G1
nzhou@uwaterloo.ca